Flagellar motility contributes to cytokinesis in *Trypanosoma brucei* and is modulated by an evolutionarily-conserved dynein regulatory system.

Ralston, Katherine S.[1], Lerner, Alana G.[1], Diener, Dennis R.[2] and Hill, Kent L.[1,3]

[1]Department of Microbiology, Immunology, and Molecular Genetics, University of California, Los Angeles, CA 90095
[2]Department of Molecular, Cellular and Developmental Biology, Yale University, New Haven, CT 06520
[3]Molecular Biology Institute, University of California, Los Angeles, CA 90095

Please address all correspondence to:
Kent L. Hill, Ph.D.
Department of Microbiology, Immunology and Molecular Genetics
University of California, Los Angeles
609 Charles E. Young Drive
Los Angeles, CA 90095
Tel: 310-267-0546
Fax: 310-206-5231
email: kenthill@mednet.ucla.edu

Running Title: Trypanin is part of the DRC
Key Words: Dynein, DRC, Motility, Trypanin, Radial Spokes, Central Pair, Chlamydomonas reinhardtii

ABSTRACT

The flagellum of *Trypanosoma brucei* is a multifunctional organelle with critical roles in motility and other aspects of the trypanosome lifecycle. Trypanin is a flagellar protein required for directional cell motility but its molecular function is unknown. Recently, a trypanin homologue in *Chlamydomonas reinhardtii* was reported to be part of a dynein regulatory complex (DRC) that transmits regulatory signals through central pair microtubules and radial spokes to axonemal dynein. DRC genes were identified as extragenic suppressors of central pair and/or radial spoke mutations. We used RNAi to ablate expression of radial spoke (RSP3) and central pair (PF16) components individually or in combination with trypanin. Both *rsp3* and *pf16* single knockdown mutants are immotile with a severely defective flagellar beat. In the case of *rsp3, this loss of motility is correlated with loss of radial spokes, while in the case of pf16, loss of motility correlates with aberrant orientation of central pair microtubules within the axoneme.* Genetic interaction between trypanin and PF16 is demonstrated by the finding that loss of trypanin suppresses the *pf16* beat defect, indicating that the DRC represents an evolutionarily-conserved strategy for dynein regulation. Surprisingly, we discovered that four independent mutants with impaired flagellar beat all fail in the final stage of cytokinesis, indicating that flagellar motility is necessary for normal cell division in *T. brucei*. These findings *present the first evidence that flagellar beating is important for cell division and* open the opportunity to exploit enzymatic activities that drive flagellar beat as drug targets for the treatment of African sleeping sickness.

INTRODUCTION

African trypanosomes are parasitic protozoa that are infectious to humans and a broad range of animals. *Trypanosoma brucei* is transmitted by the Tsetse fly and is the causative agent of African trypanosomiasis in humans, also known as "African sleeping sickness". Since *T. brucei* is an extracellular pathogen, the parasite relies on its own cell motility throughout its lifecycle, in both insect and mammalian hosts (18). In the insect vector, the parasite makes an ordered series of migrations through specific compartments to complete the developmental changes necessary for survival in a mammalian host (66, 68). In mammalian hosts, *T. brucei* initially replicates in the bloodstream, but eventually penetrates the blood vessel endothelium and invades the connective tissues and central nervous system where it initiates events that are ultimately lethal (42, 45). If untreated, African sleeping sickness is 100% fatal, and the lethal course of the disease is directly linked to the presence of parasites in the central nervous system (42, 45). Thus, parasite migration to specific host tissues correlates directly with pathogenesis.

The driving force for cell motility in *T. brucei* is a single flagellum, which extends from the basal body, through the flagellar pocket and along the length of the cell body to which it is attached (17, 67). The *T. brucei* flagellar apparatus includes a canonical eukaryotic 9+2 axoneme and additional structures, such as the paraflagellar rod (PFR) and flagellum attachment zone (FAZ), which are unique to trypanosomes and a few closely related protozoa (9, 17). Within the eukaryotic axoneme, it is well established that ATP-dependent dynein motors drive sliding of adjacent outer doublet microtubules, providing the force for flagellar movement (11, 57). To generate complex flagellar waveforms, the activity of these dynein motors must be precisely coordinated both temporally and spatially, since simultaneous activation of all dynein arms

would lead to a rigor-like state (11, 57). Dynein activity must also be coordinated with environmental sensory perception, since changes in flagellar beat form, such as wave reversal and hyperactivated motility, are often associated with physiological responses to environmental cues (32, 36, 64). Identification of proteins and mechanisms underlying dynein regulation is one of the major challenges in cell biology.

In *T. brucei*, beating of the flagellum initiates at the distal tip and is propagated toward the base, pulling the cell forward in an auger-like spiraling motion with the flagellar tip leading (Supplemental Video 1) (18, 69, 70). This implies the need for specialized dynein regulatory inputs, because in most other organisms the flagellar beat propagates from the base to the tip (22). In some trypanosomatids, flagellar beat direction is reversible and modulated in response to extracellular cues (23, 64). In addition to its role in cell motility, the trypanosome flagellum is required for attachment to epithelial cells in the Tsetse fly salivary gland (68) and plays structural roles in organelle inheritance, establishment of cell polarity and cleavage furrow formation (28, 37, 38, 52, 53). Thus, the trypanosome flagellum is a complex and dynamic organelle with critical roles throughout the parasite lifecycle. Unfortunately, our current understanding of the *T. brucei* flagellum is primarily restricted to a few major structural proteins and very little is known about proteins that regulate flagellar beat. Given the importance of motility and the flagellar apparatus in *T. brucei* development and disease pathogenesis, this represents a critical gap in our understanding of these deadly pathogens.

One protein that may play a role in regulating flagellar motility in *T. brucei* is trypanin, a 54-kDa coiled-coil protein that is tightly associated with the flagellar cytoskeleton and is required for normal flagellar motility (19, 26). Trypanin knockdown mutants have actively-beating flagella, but are unable to coordinate flagellar beat to drive productive directional motion

and are thus only able to spin and tumble in place (26). Trypanin homologues are found in most if not all organisms that contain a motile flagellum, ranging from *Giardia lamblia* to humans, but are absent in organisms that lack motile cilia/flagella, such as *Caenorhabditis elegans*, which contains only non-motile sensory cilia (19); (KH unpublished observation).

We previously reported that *Chlamydomonas reinhardtii* contains a trypanin homolog (19). Rupp and Porter recently identified the *C. reinhardtii* trypanin homolog, PF2, *in a screen for mutants that affect* a dynein regulatory complex (DRC) that transmits signals from central pair (CP) and radial spoke (RS) complexes to axonemal dynein (55). DRC genes were originally identified through the isolation of extragenic suppressors that restore flagellar beat to CP/RS mutants without restoring the missing structures (24). Isolation of these suppressors revealed the presence of a regulatory system that controls dynein activity on at least two levels (24). One group of suppressor mutations (*sup$_{pf}$3*, *sup$_{pf}$4*, *sup$_{pf}$5*, *pf2*, and *pf3*) are required for assembly of the DRC, which is localized adjacent to inner arm dynein I1 at the base of the second radial spoke in the 96 nm repeating unit of the axoneme (16, 24, 34, 43, 44). A second group of suppressors correspond to mutations in outer and inner arm dynein heavy chains (46, 47, 54). The presence of this axonemal dynein regulatory system is further supported by a variety of biochemical and ultrastructural studies (41, 61, 72). Together, these data have led to a model in which the DRC acts as a reversible inhibitor of axonemal dynein that is regulated by signals delivered via the central pair and radial spokes (48). In many organisms, the CP rotates within the axoneme and this is thought to provide a means for distributing regulatory signals to dyneins arranged around the outer doublets (40, 71, 72). In the absence of CP/RS, the DRC constitutively inhibits dynein, leading to flagellar paralysis or erratic twitching (24, 43). Loss of the DRC releases dynein inhibition, thus partially suppressing CP/RS beat defects, although suppressed

mutants do not regain wild-type motility (24, 43, 44, 48). Partial suppression reflects the fact that the DRC represents only one level of dynein regulation provided by the CP/RS system (24).

To determine if a DRC-like regulatory system operates as a conduit for transmission of regulatory signals between the CP/RS apparatus and axonemal dynein in *T. brucei*, we used RNAi to knockdown the expression of radial spoke (RSP3) and central pair (PF16) components individually, or in combination with trypanin. Our results demonstrate that radial spoke and central pair components are required for motility in *T. brucei. We also report that CP microtubules exhibit a fixed orientation relative to outer doublet microtubules in wild-type trypanosomes, while in pf16 and pf20 mutants CP orientation is highly variable.* Importantly, trypanin behaves as a DRC component since loss of trypanin suppresses the flagellar beat defect of a central pair mutant. Therefore, the DRC is an evolutionarily-conserved dynein regulatory system and trypanin is a component of this system in *T. brucei*. Surprisingly, we also discovered that flagellar motility is required for cytokinesis in *T. brucei*, as motility mutants defective in three distinct flagellar substructures all *have difficulty completing* cytokinesis.

MATERIALS AND METHODS

Cell Culture and Transfection

Procyclic culture form (PCF) 29-13 cells, which stably express T7 RNA polymerase and tetracycline (tet) repressor (74), were used to generate all RNAi knockdown mutants. Trypanosomes were cultivated and stably-transfected as described previously (20, 26). Clonal cell lines were obtained by limiting dilution. Clonal lines harboring the RNAi constructs p2T7^{-Ti-B}/RSP3, p2T7^{-Ti-B}/PF16, p2T7^{-Ti-B}/PF20, p2T7^{-Ti-B}/PFR2-1, p2T7^{-Ti-B}/PFR2-2, p2T7^{-Ti-B}/TPN, p2T7^{-Ti-B}/RSP3-TPN, or p2T7^{-Ti-B}/PF16-TPN (see DNA Constructs, below) are referred to as TbRSP3, TbPF16, TbPF20, TbPFR2-1, TbPFR2-2, TbTPN, TbRSP3/TPN, and TbPF16/TPN, respectively. For tetracycline induction, cells were split into two flasks and cultured with or without 1 μg/ml tetracycline and diluted as necessary to maintain exponential growth. For growth curves, cell densities were measured using a hemocytometer and averages of two independent counts are reported. For knockdown mutants, clusters of up to four distinguishable cell bodies were counted. To culture cells with physical shaking, TbRSP3 cells were split into flasks with or without tetracycline and placed on an orbital shaker set at 80 revolutions per minute.

Database Searches & Multiple Sequence Alignments

C. reinhardtii protein sequences for RSP3 (accession number P12759) (73), PF16 (accession number AAC49169.1) (59) and PF20 (accession number AAB41727.1) (60) were used to identify homologues in the *T. brucei* genome database (http://www.sanger.ac.uk/cgi-bin/blast/submitblast/ t_brucei/omni) using WU-BLAST (Washington University, Saint Louis,

MI). Sequencing of the *T. brucei* genome was accomplished as part of the Trypanosoma Genome Network with support by The Wellcome Trust). We identified single copy genes for RSP3 (GeneDB ID Tb11.47.0034), PF16 (GeneDB ID Tb927.1.2670) and PF20 (GeneDB ID Tb10.61.2920). The percent similarity of each *T. brucei* protein to its *C. reinhardtii* homologue is as follows: RSP3 (41.5% identity and 52.5% similarity); PF16 (55.9% identity and 69.2% similarity); and PF20 (37.3% identity and 50.6% similarity).

Multiple sequence alignments were performed with the Clustal W algorithm (65) using Vector NTI software (Vector NTI Advance Suite 8, InforMax Inc., Bethesda, MD). For RSP3, the following proteins were aligned: *Homo sapiens* (accession number AAK26432), *C. reinhardtii* (accession number P12759), *T. brucei* (GeneDB ID Tb11.47.0034), *T. cruzi* (GeneDB ID Tc00.1047053506721.20), and *Leishmania major* (GeneDB ID LmjF27.0520). For PF16, the following proteins were aligned: *H. sapiens* (accession number CAH72210), *C. reinhardtii* (accession number AAC49169.1), *T. brucei* (GeneDB ID Tb927.1.2670), *T. cruzi* (GeneDB ID Tc00.1047053510955.40), and *L. major* (GeneDB ID LmjF20.1400). For PF20, the following proteins were aligned: *H. sapiens* (accession number AAM63956), *C. reinhardtii* (accession number AAB41727.1), *T. brucei* (GeneDB ID Tb10.61.2920), *T. cruzi* (GeneDB Tc00.1047053511277.340), and *L. major* (GeneDB ID LmjF18.0470).

DNA Constructs

All RNAi plasmids were constructed in p2T7^{-Ti-B}, which contains opposing, tetracycline-inducible T7 promoters such that tetracycline-induced transcription generates an intermolecular double stranded RNA (dsRNA) (30). To create p2T7^{-Ti-B}/RSP3, a 375-bp fragment corresponding to nt 566 – 940 of the *T. brucei* RSP3 ORF was PCR-amplified from 29-13

genomic DNA and cloned in the forward orientation into the *Hin*dIII and *Sac*II sites in p2T7$^{-Ti\text{-}B}$. To create p2T7$^{-Ti\text{-}B}$/PF16, a 247-bp fragment corresponding to nt 1288 – 1534 of the *T. brucei* PF16 ORF was PCR-amplified from 29-13 genomic DNA and cloned in the forward orientation into the *Sac*II and *Xba*I sites in p2T7$^{-Ti\text{-}B}$. To create p2T7$^{-Ti\text{-}B}$/PF20, a 407-bp fragment corresponding to nt 291 – 697 of the *T. brucei* PF20 ORF was PCR-amplified from 29-13 genomic DNA and cloned in the forward orientation into the *Sac*II and *Xba*I sites in p2T7$^{-Ti\text{-}B}$. To create p2T7$^{-Ti\text{-}B}$/PFR2-1, a 448-bp fragment corresponding to nt 642 – 1089 of the *T. brucei* PFR2 ORF (GeneDB ID Tb08.5H5920) was PCR-amplified from 29-13 genomic DNA and cloned in the forward orientation into the *Hind*III and *Bam*HI sites in p2T7$^{-Ti\text{-}B}$. Note that this fragment of PFR2 was selected by RNAit (49) and is not expected to target PFR1 (GeneDB ID Tb03.26J7510) mRNA, since it does not contain any regions of identity to PFR1 longer than 12 nt. To create p2T7$^{-Ti\text{-}B}$/PFR2-2, a 1723-bp fragment corresponding to nt 78 – 1800 of the *T. brucei* PFR2 ORF was PCR-amplified from 29-13 genomic DNA and cloned in the forward orientation into the *Hind*III and *Bam*HI sites in p2T7$^{-Ti\text{-}B}$. This fragment of PFR2 is identical to the fragment used to create the *snl*-2 cell line (4), and is similar to the fragments used to create *snl*-1 (nt 78 – 1758) (7) and PFRAi (nt 78 –1779) (14). To create p2T7$^{-Ti\text{-}B}$/TPN, a 252-bp fragment corresponding to nt 1103 – 1354 of the *T. brucei* trypanin ORF (26) was PCR-amplified from 29-13 genomic DNA and cloned in the forward orientation into the *Bam*HI and *Hin*dIII sites in p2T7$^{-Ti\text{-}B}$. All RNAi constructs were verified by restriction digestion and direct sequencing. Plasmids were linearized at the unique *Eco*RV or *Not*I site for transfection.

To create dual RNAi knockdown plasmids, tandem fragments of the targeted genes were cloned into p2T7$^{-Ti\text{-}B}$. To construct p2T7$^{-Ti\text{-}B}$/RSP3-TPN, the precise 375-bp RSP3 fragment that was used to create p2T7$^{-Ti\text{-}B}$/RSP3 was cloned in the forward orientation into the *Xba*I and

*Bam*HI sites, upstream of the TPN fragment in p2T7$^{-Ti\text{-}B}$/TPN. To create p2T7$^{-Ti\text{-}B}$/PF16-TPN, the precise 247-bp PF16 fragment that was used to create p2T7$^{-Ti\text{-}B}$/PF16 was cloned in the forward orientation into the *Xba*I and *Bam*HI sites, upstream of the TPN fragment in p2T7$^{-Ti\text{-}B}$/TPN.

RNA Preparation and Northern Blotting

Total RNA samples were prepared using an RNeasy kit (Qiagen) according to the manufacturer's instructions. RNA samples (5 μg) were analyzed by Northern blotting as described previously (21). ^{32}P-labeled probes corresponding to nt 198 – 546 of the RSP3 ORF ("RSP3 Probe"), nt 1288 – 1534 of the PF16 ORF ("PF16 Probe"), nt 291 – 697 of the PF20 ORF ("PF20 Probe"), nt 642 – 1089 of the PFR2 ORF ("PFR2 Probe"), nt 1 – 775 of the TPN ORF ("TPN Probe"), or the entire TRP ORF ("TRP Probe") were used. The TRP gene (GeneDB ID Tb09.244.2800) encodes a "Trypanin-Related Protein" with 28% identity and 43% similarity to trypanin and will be described elsewhere (KH, unpublished observation).

Sedimentation Assays

Sedimentation assays were performed as described (6). Briefly, cells were incubated with or without tetracycline for 24 hours and then resuspended to 5x10^6 cells/ml in fresh medium. Each culture was aliquoted into four cuvettes (1 ml per cuvette) and incubated under standard growth conditions. The optical density at 600 nm (OD600) was measured every two hours. At each time point, two cuvettes from each culture were left undisturbed to monitor sedimentation while the other two cuvettes were resuspended to monitor growth. The ΔOD600 for each sample was calculated by subtracting the OD600 of resuspended samples from undisturbed samples.

Protein Preparation and Western Blotting

Protein extracts were prepared and analyzed by Western blotting (20). Trypanin was detected with a monoclonal antibody directed against a synthetic peptide corresponding to the last 13 amino acids of trypanin and was generated by an outside vendor (Cell Essentials, Cambridge, MA). PFR2 was detected with the monoclonal antibody L8C4 (29). The monoclonal antibody E7, directed against β-tubulin, was used as a control for protein loading. This antibody was developed by (10) and obtained from the Developmental Studies Hybridoma Bank maintained by the University of Iowa Department of Biological Sciences.

Cell Imaging

Live cells were imaged using a Zeiss Axiovert 200M inverted microscope with a 63X Achroplan LD, or 63X Plan-neofluor oil-immersion objective. Video images were captured as described below. For fluorescence microscopy, cells were imaged on a Zeiss Axioskop II compound microscope with a 63X Plan-neofluor oil-immersion objective and images were captured using a Zeiss Axiocam digital camera and Zeiss Axiovision 3.0 software.

Electron Microscopy

TbRSP3, TbPF16 and TbPF20 cells were grown in the presence or absence of 1 μg/ml tetracycline (96 hours for TbRSP3 or 60 hours for TbPF16 and TbPF20). Cytoskeletons or whole cells were prepared (19, 51) then fixed for 60 minutes as described (26) with the addition of 1% (weight/vol) tannic acid. Samples were then washed in fixative without tannic acid and

shipped overnight to Yale University where processing was completed according to (58), except that staining *en bloc* was in 2% uranyl acetate for 2 hours.

Cytoskeletons were used for radial spoke analysis. Since a full complement of nine radial spokes was not always visible in all control sections, we established a blind assay to compare tetracycline-induced *rsp3* mutants to uninduced controls. Random silver sections from control (- Tet, n = 32) and tetracycline-induced (+ Tet, n = 31) samples were scanned for axonemes in which the central pair microtubules were cut in cross section. These axonemes were photographed, the images were coded, then mixed and scored blindly to determine the number of spokes present per axoneme. After scoring, samples were decoded, divided into control and tetracycline-induced groups and the data are reported as the number of sections in each group having 0 – 9 spokes per section.

Whole cell samples were used to measure the orientation of central pair microtubules in control cells and *pf16* and *pf20* mutants. Samples were selected randomly in which at least four outer doublet microtubules were clearly resolved. To measure central pair orientation, a reference line was drawn from the center-point of outer doublet one to the center-point of outer doublet seven. Outer doublet seven can be readily identified by its attachment to the PFR (5). A line was then drawn that bisects the C1 and C2 central pair microtubules and the angle of intersection of this line with the reference line was measured, moving clockwise from the reference line. The median angle in 45 control cells was 72 degrees. For reference, this angle (72 degrees) was set to zero and the data were plotted as degrees deflection from zero.

Cell Viability Assay

TbRSP3 cells were incubated with or without tetracycline for 26 hours and then subjected to a dye-exclusion assay for cell viability (Molecular Probes Live/Dead Assay #L-3224) according to the manufacturer's instructions. Briefly, cells were washed once, resuspended to $2x10^7$ cells/ml in 1X PBS, and 50 µl of cells were then added to uncoated glass coverslips and incubated in 5 µM ethidium homodimer-1 in 1X PBS for 30 minutes. Coverslips were inverted onto glass slides, sealed with nail polish and imaged.

Immunofluorescence Assays

To follow cell cycle progression, cytoskeletons were prepared by detergent-extraction (51) and subjected to immunofluorescence as described previously (26) using the α-PFR2 monoclonal antibody L8C4 (29). Anti-mouse secondary antibodies conjugated to Alexa-Fluor488 (Molecular Probes) were used at a 1:400 dilution. Samples were mounted in Vectashield H-1200 (Vector Labs), containing 1.5 µg/ml 4',6-diamidino-2-phenylindole (DAPI) to visualize kinetoplast and nuclear DNA, and then imaged. Cell cycle analysis was performed as described (58). Cells were distinguished as having one or two flagella (1F/2F), one or two kinetoplasts (1K/2K), and one nucleus or two discrete nuclei (1N/2N). A separate category (1mN) was used to distinguish cells with mitotic nuclei that contained a visible spindle. To minimize the influence of downstream defects, cells were examined 30 - 48 hours post-induction, which corresponded to the onset of the cytokinesis defect.

Quantitation of Cytokinesis in Live Cells

Live TbRSP3 cells, grown in the presence (+Tet, n = 792) or absence (-Tet, n =676) of 1 μg/ml tetracycline for 48 hours were analyzed at the same cell densities in logarithmic growth and two separate samples were quantified for each culture (+Tet, n = 393 and n = 399; -Tet, n = 334 and n = 342), with standard deviation indicated by error bars. *Note that the number of cells in cytokinesis was much higher in live cultures than in cells processed for immunofluorescence or harvested for routine cell counting. This indicated that cells undergoing cytokinesis were easily separated by physical manipulation. To account for this, live cultures were directly examined in culture flasks with minimal physical manipulation.* Cells were categorized as having a single cell body, or multiple physically attached cell bodies. Cells in which two cell bodies remain attached to one another ("double" in Figure 4B) were further subdivided into three categories. "Double-1" corresponded to cells that had two full-length flagella, but had not visibly begun cytokinesis (stage VI – VIII, as defined in Figure 31 of (58)). "Double-2" corresponded to cells that were in the middle-to-late stages of cytokinesis (stage IX (58)), while "double-3" corresponded to cells in the final stage of cytokinesis that were attached only by their extreme posterior ends (stage X (58)). Note that cells in each of these stages were also present in wild-type cultures (Figure 4B) (58) and are therefore normal events in the *T. brucei* cell division cycle. The data shown are representative of three independent experiments.

Video Microscopy of Live Cells

Videos can be accessed at http://www.mimg.ucla.edu/faculty/Hill/videos.htm , user_id: videos, password: hill_lab. *pf16* single and *pf16/tpn* double mutants (TbPF16 and TbPF16/TPN cells, respectively) were examined 48 hours post-induction using differential interference contrast (DIC) optics. Cells were visualized on standard glass slides, with double-sided tape

between the slides and coverslips creating a chambered space to allow freedom of movement. Slides were inverted and examined through the coverslip. Videos were imaged using a COHU CCD analog video camera and converted to digital format with a HandyCam (Sony, Inc.). Digital clips were captured at 30 frames per second and converted to AVI movies with Adobe Premiere Elements software (Adobe Systems). Representative examples are shown in the Supplemental Videos to illustrate the major phenotypes of each mutant. In Figure 4A, images shown are single frames from Supplemental Videos 6 – 7. In Figure 5C, images shown are single frames from Supplemental Videos 9 and 10. In Figure 8, images shown in panels A and B are frames from Supplemental Videos 3 and 11, respectively. Frames were rotated to orient posterior end of the cell body upward.

Flagellar Beat Analysis

DIC video of live *pf16* single and *pf16/tpn* double mutants (TbPF16 and TbPF16/TPN cells, respectively) was captured 48 hours post-induction as described above. For each cell line, footage of 100 random cells was recorded and analyzed. Since flagellar beat in *T. brucei* is three-dimensional and bending can occur independently in the distal and proximal portions of the flagellum, it is difficult to reliably measure frequency and amplitude of a single waveform along the length of the entire flagellum. Therefore, we measured the number of beats in each mutant over a ten second period, focusing on the flagellar tip, where single mutants are most active. Beats of the flagellar tip were quantified over a 10 second time period for each cell. Where cells exhibited more than 12 beats in 10 seconds, individual flagellar movements could not be quantified, and these cells were categorized as ">12" beats/10 seconds, which is essentially continuous movement. An example of a *pf16* mutant that had >12 movements in this assay is

shown in Supplemental Video 4 to illustrate the qualitative differences between *pf16* and *pf16/tpn* mutants in the >12 category (see Figure 8C).

RESULTS

RSP3, PF16, and PF20 are required for flagellar motility

We used RNAi to target radial spokes and the central pair apparatus of *T. brucei*. To target radial spokes, we chose RSP3, which is required for attachment of the spoke to the axoneme in *C. reinhardtii* (12). The major components of the central pair apparatus are two singlet microtubules, C1 and C2, together with their specific projections and intermicrotubule bridges (62). To target the central pair apparatus we chose PF16 and PF20, which are localized to the C1 and C2 microtubule structures, respectively (59),(60), and are required for stability of central pair microtubules in *C. reinhardtii* (1, 15) *and mice (56, 76).*

BLAST searches of the *T. brucei* genome database identified single-copy RSP3, PF16 and PF20 homologues (Materials and Methods). Protein alignments demonstrated that these proteins are highly conserved, with PF20 exhibiting the most divergence (Figure 1). In the region of overlap, the percent identity among RSP3, PF16 and PF20 homologues are 27.9%, 42.4% and 16.7%, respectively. The *C. reinhardtii* and human RSP3 proteins have unique C-terminal extensions of 201 and 90 amino acids, respectively, while the *C. reinhardtii* PF16 protein has a unique C-terminal extension of 52 amino acids, suggesting some aspects of their function may be organism-specific. Notably, a shorter C-terminus is also observed in RSP3 and PF16 from other kinetoplastids (Figures 1A and B) and deletion studies in *C. reinhardtii* indicate that the C-terminal 140 amino acids of RSP3 are not required for motility (13).

Separate plasmids for tetracycline-inducible RNAi knockdown of RSP3, PF16 and PF20 were constructed and stably-transfected clonal cell lines were obtained by limiting dilution. These cell lines will be henceforth referred to as “TbRSP3,” “TbPF16,” and “TbPF20” cells or

interchangeably as *rsp3*, *pf16* and *pf20* knockdown mutants. Northern blot analysis demonstrates that the targeted transcripts are dramatically reduced within 24 hours of tetracycline-induction (Figure 2A). Likewise, visual inspection of *rsp3*, *pf16* and *pf20* knockdown mutants revealed a severe motility defect within 24 hours of induction (see below). To quantitate this defect we performed sedimentation assays (Figure 2B). All three mutants sedimented at a linear rate of approximately -0.03 OD600 units/hour, while uninduced cells remained suspended. A dye-based viability assay demonstrated that there was no difference in viability at the time of the assay (Materials and Methods).

Close examination revealed that *rsp3*, *pf16* and *pf20* knockdown mutants were immotile in the sense that they exhibited no net movement in any direction, nor did they rotate or tumble as observed for trypanin knockdown mutants (26). However, a rudimentary flagellar beat or twitching was observed in all three mutants, so these cells should be considered "immotile", but not "paralyzed". This was particularly evident in *rsp3* mutants, where a few cells were completely paralyzed, but most were able to sustain a rudimentary flagellar beat (Supplemental Video 2). Nonetheless, flagellar movement was generally confined to the distal portion of the flagellum, was mostly planar and did not drive rotation of the cell body. Electron microscopy demonstrated that the number of spokes is reduced in axonemes of *rsp3* mutants *compared to controls* (Figure 2C *and D*). *In control cells, six or more spokes were clearly visible in 74% of sections (n = 32), compared to only 25% of sections from rsp3 mutants (n = 31). The average number of spokes per section was reduced to 4.2 in rsp3 mutants compared to 6.6 in controls.*

pf16 and *pf20* mutants were also immotile and incapable of cellular rotation (Supplemental Videos 3 and 5). However, the beat defect was more severe than in *rsp3* mutants (compare Supplemental Videos 3 and 5 with Video 2). Whereas *rsp3* mutants were able to

sustain a modest flagellar beat, *pf16* and *pf20* mutants only twitched erratically and this irregular twitching was confined to the distal region of the flagellum. An additional feature shared by *pf16* and *pf20* mutants, but not *rsp3* mutants, was an exaggerated curvature in the cell body such that the flagellum tip and the anterior end of the cell were bent in an "S" shape toward the side of the cell opposite the flagellum (Supplemental Videos 3 and 5 and Figure 8A). In these cells, the flagellum was situated along the outer edge of the bend, such that flagellar movement decreased the degree of bending, but was not powerful enough to fully straighten the cell body.

Electron microscopy of *pf16* and *pf20* mutants (Figure 3) demonstrated a striking alteration in the orientation of the central pair microtubules. In control cells, central pair orientation within the axoneme was found to be restricted to a very narrow range, such that a plane bisecting the C1 and C2 microtubules was always roughly parallel to the paraflagellar rod viewed in cross-section (Figures 3A and 3C). In contrast, orientation of the central pair was *highly variable* in *pf16* and *pf20* mutants (Figures 3B and 3C). *Since we cannot distinguish between the two central pair microtubules, we do not know if this represents random orientation through 360 degrees, or only 180 degrees.*

Flagellar motility is required for cytokinesis

RNAi knockdown of RSP3, PF16 and PF20 resulted in a severe motility defect that was evident within 24 hours of tetracycline-induction. Surprisingly, in all three mutants loss of motility was invariably followed by a cell division defect *such that cells failed to complete normal cell division* and accumulated as clusters attached at their extreme posterior ends (Figure 4A and Supplemental Videos 6 – 7). *Cleavage furrow formation in T. brucei initiates at the anterior end of the cell, between the tips of the new and old flagella, then proceeds toward the*

posterior end and in the final stages of cytokinesis daughter cells are only connected at their posterior ends (58). *In wild type cells, these daughter cells eventually pull apart before the next round of cytokinesis, while the motility mutants do not, and therefore accumulate as larger and larger clusters.* This defect was investigated more thoroughly in *rsp3* mutants, where reduced severity of flagellar paralysis allowed us to examine early *aspects of the phenotype*. Within 48 hours post-induction, there was a decrease in the number of single cells and an increase in cell clusters containing two, three, four, and more than four conjoined cell bodies. Among the "double" cells (as defined in *Materials and Methods* and Figure 4), there was no significant change in cells that had not initiated cytokinesis (Figure 4B, "double-1"), while there was a significant increase in cells in the middle to late stages of cytokinesis (Figure 4B, "double-2"). There was a modest decrease in the number of "double-3" cells, perhaps indicating that cells undergoing cytokinesis must fully complete the "double-2" stage before reaching the final stage. Analysis of cell cycle progression by immunofluorescence (Materials and Methods) demonstrated that, aside from cells blocked in cytokinesis, there was no accumulation at any other stage of the cell cycle (not shown). These data, together with the fact that new rounds of cytokinesis can be initiated in "double" cells to produce "triple" and "quad" clusters, indicated that initiation of cytokinesis was not significantly affected, but that daughter cells were unable to complete cell separation.

Knockdown of three different axonemal proteins resulted in loss of cell motility and a concomitant cytokinesis defect. Since the cytokinesis defect was unexpected, we asked whether a similar defect would be observed when we targeted a non-axonemal protein that is required for normal cell motility. PFR2 is one of two major proteins that comprise the kinetoplastid paraflagellar rod (5). Previously described PFR2 knockdown mutants had reduced flagellar beat

and were immotile at the cellular level (4, 7). These mutants exhibited a reduced growth rate compared to wild-type (6), although no specific cytokinesis defect was reported. To further investigate the connection between flagellar beat and cytokinesis, we generated two independent, tetracycline-inducible PFR2 knockdown mutants. Tetracycline induction led to a rapid and dramatic loss of PFR2 mRNA and protein in both mutants (Figure 5A and B). The flagella of these mutants were able to beat, but beating was not sufficient to drive directional cell motility or significant cellular rotation (Supplemental Video 8). Within 24 hours of tetracycline induction, *pfr2* mutants began to accumulate as small clusters of cells attached at their posterior ends (Figure 5C; Supplemental Videos 9 and 10), and a reduction in growth rate was observed (Figure 5E). By four days post-induction, the majority of cells accumulated in massive clusters (Figure 5D). Therefore, as was the case for central pair and radial spoke proteins, loss of PFR2 led to reduced flagellar beat, loss of cell motility and a concomitant block in cytokinesis.

Failure to complete cytokinesis in four independent motility mutants might reflect an active requirement for flagellar beat. Alternatively, the effect might be indirect, with impaired beat causing internal structural defects that prevent separation of daughter cells. If flagellar beat contributes directly to cell separation, gentle agitation of mutant cultures may provide compensatory forces that allow cell division. On the other hand if the effect *is simply indirect, i.e. flagellar paralysis simply distorts something inside the cell and as a result cells are inextricably intertwined*, agitation is not expected to correct these defects and clusters should still form. Growth rate and cytokinesis were examined in motility mutants maintained normally ("unshaken") or on a rotating platform ("shaken"). Rotation of the culture completely rescued the cytokinesis defect, restored growth rate (Figure 6A) and prevented formation of multicellular clusters (Figure 6B).

Trypanin functions as part of a DRC in *T. brucei*

The motivation for generating radial spoke and central pair mutants was to determine whether a dynein regulatory system provides communication between CP/RS and axonemal dynein in *T. brucei*. The defining feature of DRC genes is that loss-of-function mutations in these genes suppress flagellar beat defects of central pair and radial spoke *loss-of-function* mutants (24). Tetracycline-inducible *pf16/tpn* and *rsp3/tpn* dual RNAi knockdown mutants were generated as described in Materials and Methods. Northern blot (Figure 7A and B) and Western blot (Figure 7C) analyses demonstrated that knockdown in double mutants was as efficient as knockdown in the corresponding single mutants.

The motility defect of *rsp3* and *pf16* single mutants in *T. brucei* is defined by three shared phenotypic characteristics: i) sedimentation; ii) an abnormal flagellar beat that is often restricted to the flagellar tip; iii) cytokinesis failure. Additionally, flagellar beat in *pf16* mutants is restricted to an erratic twitching, resulting in a sharp curvature in the anterior cell body. The ability of trypanin knockdown to suppress any or all of these phenotypic characteristics was determined. Loss of trypanin did not suppress overall cellular movement defects, since the growth rate and sedimentation profiles of double mutants were similar to single mutants (not shown). However, the key feature of DRC suppression is improved flagellar beat, which was therefore examined with high-resolution phase contrast and differential interference contrast (DIC) microscopy. While the less severe phenotype of *rsp3* mutants made it difficult to reliably detect improved flagellar beat, suppression of the *pf16* beat defect was immediately obvious in *pf16/tpn* double knockdown mutants (Figure 8A and B, Supplemental Videos 11 and 12). In contrast to the erratic flagellar twitch exhibited by *pf16* single mutants, *pf16/tpn* double mutants

produced a sustained flagellar waveform and rarely twitched (compare Supplemental Videos 11 and 12 with Video 3). Likewise, curvature of the anterior cell body and flagellum, which is a hallmark of *pf16* single mutants, was reduced or absent in double mutants (Figures 8A and 8B), most likely as a direct result of the more regular and controlled beating of the flagellum.

To demonstrate the suppression afforded by loss of trypanin, the phenotypic characteristics of these mutants were used to distinguish *pf16* single and *pf16/tpn* double mutants in a blind assay. Fifty separate samples of *pf16* and *pf16/tpn* mutants were visually inspected and mutants were accurately identified as single (*pf16*) or double (*pf16/tpn*) (Table 1). We also performed a quantitative analysis of flagellar motion to distinguish single and double mutants (Figure 8C). One hundred *pf16* single mutants and one hundred *pf16/tpn* double mutants were examined and this analysis showed that flagella of most double mutants beat continuously, while single mutants do not (Figure 8C). Therefore, loss of trypanin suppresses the erratic twitching and curved flagellum that are hallmarks of *pf16* mutants.

DISCUSSION

The *T. brucei* flagellum is important for many aspects of trypanosome cell biology and host-parasite interaction, yet our knowledge of the trypanosome flagellar apparatus is limited. In this study, we advance understanding of this organelle in *four* important ways. First, we establish a requirement for central pair and radial spoke components in *T. brucei* motility. *Second, we demonstrate for the first time that orientation of CP microtubules is fixed relative to outer doublet microtubules and that* and that abnormal central pair orientation is correlated with severely defective motility. *Third*, our results demonstrate that flagellar motility is *contributes* to normal cytokinesis in *T. brucei* and suggest that the flagellum has an active role in cell division, beyond its passive role as a structural and positional cue. Finally, we provide genetic evidence that the dynein regulatory complex, previously characterized only in algae, represents an evolutionarily-conserved strategy for dynein regulation and that trypanin operates together with PF16 in a DRC-like regulatory system in *T. brucei*.

Trypanin is part of an evolutionarily-conserved dynein regulatory system

Many cellular functions are dependent upon correct spatial and temporal regulation of dynein motors and identification of proteins and mechanisms underlying this regulation represents a major challenge in cell biology. In *C. reinhardtii,* the DRC functions as part of a mechanochemical signal transduction pathway that regulates axonemal dynein in response to signals from central pair microtubules and radial spokes (24, 43, 44, 55). DRC components are defined through their genetic interaction with central pair components. Specifically, loss of function DRC mutations suppress flagellar beat defects of central pair loss of function mutants

(24). Using dual RNAi knockdown, we show that loss of trypanin suppresses flagellar beat defects of a central pair (*pf16*) knockdown mutant in *T. brucei*, demonstrating a genetic interaction between trypanin and PF16. Therefore, trypanin meets the following criteria of a DRC component: 1) trypanin loss suppresses a central pair beat defect without restoring expression of the central pair protein; 2) trypanin single knockdown mutants exhibit a motility defect indicative of abnormal dynein regulation (26); 3) trypanin is stably associated with flagellar axonemes (19); and 4) is distributed along the length of the flagellum (26). Taken together, these data show that trypanin functions as part of a DRC-like regulatory system in African trypanosomes. Although we did not readily detect a genetic interaction between RSP3 and trypanin, this is probably because the less severe *rsp3* phenotype makes suppression too subtle to detect.

Trypanin single knockdown mutants are incapable of directional cell motility, but have an actively beating flagellum and are able to spin and tumble in place (26). Interestingly, a tumbling motion similar to the trypanin knockdown phenotype is also observed transiently in wild-type cells as they alternate between directional runs and random tumbles (18, 26). Therefore, the DRC of trypanosomes may provide a clutch-like regulatory mechanism that can be engaged for directional movement, or disengaged for random tumbling. In bacteria, this type of behavior is exploited to drive changes in taxis in response to environmental cues (33).

A DRC function for trypanin is also supported by the localization of trypanin along the flagellum and may explain the flagellum attachment defect of trypanin knockdown mutants. The *T. brucei* flagellum is directly connected to the cell body along its length and trypanin knockdown mutants exhibit partial flagellar detachment (26). This defect is more pronounced upon removal of cellular membranes, suggesting that loss of trypanin compromises the structural

integrity of flagellum attachment complexes (26). Since the DRC functions in beat regulation, flagellum detachment in *tpn* knockdown mutants might be an indirect consequence of the motility defect, as previously suggested (55), rather than a direct consequence of the loss of trypanin. These two explanations are not mutually exclusive, and a third possibility is that trypanin functions in both capacities. The 96 nm periodicity of the DRC along the axoneme in *C. reinhardtii* (16), is the same as the periodicity of flagellum attachment complexes in *T. brucei* (67). Therefore, the DRC or an associated structure might be exploited to serve a secondary function as an axonemal attachment site. Distinguishing between these possibilities will require more precise ultrastructural localization of trypanin and the DRC in *T. brucei*.

Further analysis of flagellar dynein regulation in *T. brucei* will be of tremendous interest, particularly since the trypanosome genome also contains a trypanin paralogue, "Trypanin-Related Protein" (TRP, see Materials and Methods). TRP mRNA is not targeted by trypanin RNAi (Figure 7A) and the contribution of TRP to dynein regulation remains to be determined. Interestingly, genes for both trypanin and TRP are found in other kinetoplastids, while *C. reinhardtii* and humans have only a single trypanin homologue (KH, unpublished observation). The presence of a paraflagellar rod in kinetoplastids imparts structural asymmetry to the axoneme, as outer doublets four through seven are physically linked to the paraflagellar rod (5). This asymmetric arrangement undoubtedly imposes unique regulatory demands and perhaps this need is met with two distinct dynein regulatory systems, one containing trypanin and the other containing TRP.

Radial spoke and central pair proteins are required for flagellar motility in *T. brucei*

We identified *T. brucei* RSP3, PF16, and PF20 homologues as single copy genes in the *T. brucei* genome. *Knockdown of each of these genes results in severely defective motility.* Ultrastructural analysis demonstrates *loss of radial spokes in rsp3 mutants and abnormal central pair orientation in pf16 and pf20 mutants. In vitro studies with reactivated axonemes show that position of the C1 microtubule of the central pair correlates with the position of active dyneins in C. reinhardtii (71, 72). Hence, the restricted orientation of central pair microtubules, together with aberrant central pair orientation in pf16 and pf20 mutants, supports the idea that all dyneins around the circumference of the axoneme do not receive the same regulatory inputs in T. brucei. It is possible that abnormal central pair orientation in T. brucei pf16 and pf20 mutants leads to aberrant dynein activity and abnormal motility, but currently we do not know whether abnormal central pair orientation is the cause or consequence of the motility defect.* We did not observe loss of central pair microtubules in intact cells (Figure 3) or demembranated flagella (not shown) from *pf16* or *pf20* mutants. In contrast, *pf16* and *pf20* deficiency in *C. reinhardtii* (1, 15) and mice (56, 77) manifest as instability of central pair microtubules, although the precise function of these proteins is not known. Interestingly, loss of central pair microtubules in *C. reinhardtii pf16* mutants is observed in demembranated axonemes, but not in intact cells (15), indicating that something other than absence of the central pair is responsible for the motility defect. By demonstrating that the presence of central pair microtubules is not sufficient for motility in T. *brucei*, our results also extend the findings of McKean and coworkers (35), who demonstrated that complete ablation of the central pair apparatus in *T. brucei* by gamma tubulin knockdown disrupts cell motility.

A rudimentary beat is often observed in the flagellar tip of *rsp3*, *pf16* and *pf20* mutants. Since flagellar beat in *T. brucei* initiates at the tip (69, 70), it thus appears that these mutants are

able to initiate but not propagate flagellar beat. The pronounced curvature of *pf16* and *pf20* mutants likely also results from the inability to sustain flagellar beat, since it is reduced or absent in *pf16/tpn* double mutants and *rsp3* single mutants. The twitching and curved flagellum seen in *T. brucei pf16* and *pf20* mutants is similar to the twitching and curved flagellum of sperm from *pf16* knockout mice (56) and *pf20* chimeric mice (76). Twitching and phenotypic heterogeneity is also observed in *C. reinhardtii pf16* and *pf20* loss of function mutants (1, 15), suggesting that residual flagellar movement is independent of PF16 and PF20 and is not simply due to incomplete knockdown.

Radial spokes are composed of an estimated 23 proteins (75) with a surprisingly large number containing predicted regulatory domains, supporting the emerging concept that spokes play important roles in signal transduction and are not simply structural components of the flagellum (62). The central pair apparatus is also composed of at least 23 proteins (1, 15). By establishing a requirement for radial spoke and central pair proteins in trypanosome motility, our results facilitate structure-function analyses by aiding in rational selection of key amino acids to target with site-directed mutagenesis. The repertoire of tools available for molecular genetic manipulation in *T. brucei*, including targeted gene knockouts and inducible RNAi knockdowns, makes these parasites a powerful system for elucidating function of these and other (3, 31) candidate motility genes.

Flagellar motility is required for cytokinesis

An unanticipated finding from our studies is that flagellar motility is required for normal cell division. *rsp3*, *pf16*, *pf20* and *pfr2* knockdown mutants are each blocked at the final stage of cell separation, but can reinitiate cytokinesis multiple times. Loss of RSP3, PF16, PF20 or PFR2 affects distinct substructures within the flagellum and in all four mutants defective flagellar

motility precedes the block in cytokinesis. Therefore, flagellar motility itself, rather than a specific flagellar substructure, is required for cytokinesis.

Other motility mutants have been described in *T. brucei*. Since those that are nonviable are also defective in critical structures such as the mitotic spindle (35), or flagellum attachment zone (28, 30), it is difficult to assess the relative contribution of flagellar beat to the lethal phenotype. PFR2 knockdown mutants, *snl-1* (7) and *snl-2* (4), have been described previously that exhibit severely reduced flagellar beat. These mutants are viable, but grow more slowly than wild type (6). Cytokinesis was not specifically examined in the previous studies, although one report indicates that *snl-2* cells divide normally (4). Re-examination of these mutants demonstrates they form multicellular clusters, albeit not to the extent seen in the *pfr2* mutants obtained in the current study (P. Bastin, personal communication). The reason for the difference in severity is not entirely clear, but both *snl-1* (7) and *snl-2* (4) were isolated under conditions in which PFR2 dsRNA is expressed. Hence, there is selective pressure for compensation to allow outgrowth of these mutants and the difference in severity may be due to differences in extent of flagellar beating and/or other compensating factors. Consistent with this explanation, transfection of the *snl-2* plasmid into a cell line that lacks a tet-repressor and therefore expresses high levels of the PFR2 dsRNA, gave poor transfection efficiency and the few transfectants obtained had severe cytokinesis defects (P. Bastin, personal communication). An independent *pfr2* mutant generated utilizing an intermolecular dsRNA is viable (14), but also forms multicellular clusters (P. Bastin, personal communication). Finally, attempts to generate a PFR2 knockout via gene disruption in *T. brucei* have failed (25), consistent with the idea that the PFR2 gene is essential. Therefore, the combined data support a requirement for flagellar motility in cytokinesis in *T. brucei.*

The cytokinesis defect of motility mutants might reflect a direct or indirect role for flagellar beat, or a combination of direct and indirect roles. Several lines of evidence suggest that a direct role is at least partially responsible. The initial defect is marked by an accumulation of cells connected at their extreme posterior ends. Hence, cleavage furrow ingression and progression along the flagellum attachment zone is normal and cell separation fails at the posterior end. Indeed, daughter cells are sometimes connected by only a thin string of membrane (data not shown). It is difficult to envision internal structural defects preventing cell separation at this stage of division. This is very different than the phenotype observed in *fla1* mutants, where disruption of flagellum attachment structures prevents initiation of cytokinesis (30). Flagellar motility can influence positioning of the kinetoplast (unpublished observation), which is connected to the flagellar basal body (39), and it is possible that indirect effects also contribute to the cytokinesis defect, particularly several days post-induction. However, the finding that *physical forces provided by* mechanical rotation of cultures completely rescues the cytokinesis defect demonstrates that no physical barrier precludes cell separation and supports the idea that physical forces provided by flagellar beat *contribute* to cell division. Mechanical forces also contribute to cytokinesis in animal cells (50). *In wild type trypanosomes at the final stage of cytokinesis, daughter cells are opposing one another with their flagella pointing in opposite directions (Video 13) (58)* .Since there is no compelling evidence for an actin/myosin II contractile ring at the cleavage furrow in *T. brucei* (15), exploiting directional and rotational pulling forces imparted by flagellar beating would be a convenient way to aid in the final separation of dividing cells. *A similar phenomenon, termed rotokinesis, whereby ciliary-driven cell motility and perhaps cell rotation assists in the separation of daughter cells, has been*

described in Tetrahymena thermophila (8). Note that a universal feature of *trypanosome* motility mutants that fail in cytokinesis is that they do not rotate. In contrast, flagellar beat drives vigorous cellular rotation in wild type cells and in trypanin single mutants, which divide normally (Table 2, compare supplemental videos 13 and 14) (26).

Summary

Defects in ciliary motility are linked to wide variety of inherited human diseases (2, 27, 63) and a better understanding of flagellar motility is critical for the development of new strategies to treat these diseases. Although structural features of the flagellum have been studied extensively and are considered to be well-conserved, regulatory mechanisms that control flagellar beat are not well understood in any organism. In the present work, we demonstrate that the DRC is an evolutionarily-conserved dynein regulatory system and that altered orientation of central pair microtubules is linked to cell motility defects *in vivo*. We also provide the first evidence that flagellar motility is required for cell division in *T. brucei*, the causative agent of African sleeping sickness. This suggests that the numerous enzymatic activities, e.g. ATPases, phosphatases and kinases (48), which drive beating of the eukaryotic flagellum represent candidate drug targets for treatment of this fatal disease.

ACKNOWLEDGEMENTS

This work was supported by grants from the National Institutes of Health (R01AI52348) and Ellison Medical Foundation (ID-NS-0148-03) to K.L.H. K.S.R. is a recipient of a USPHS National Research Service Award (GM07104). A.G.L. was supported by a MARC U*STAR traineeship from the NIH/NIGMS (GM08563). We are extremely grateful to Bryce McLelland for preparation of trypanin monoclonal antibodies and all of his excellent technical assistance and invigorating discussions. We thank Philip Postovoit and Joel Schonbrun for assistance with video imaging. We thank Dr. Philippe Bastin for stimulating discussions and sharing unpublished work, Dr. Keith Gull for antibodies against PFRA, Dr. George Cross for the 29-13 cell line and Dr. John Donelson for the p2T7-Ti plasmid. We thank Dr. Nancy Sturm for many helpful and stimulating discussions on the manuscript and are grateful to colleagues and members of our laboratory for critical reading of the manuscript and thoughtful comments on the work.

REFERENCES

1. ***Adams, G. M., B. Huang, G. Piperno, and D. J. Luck.*** *1981. Central-pair microtubular complex of Chlamydomonas flagella: polypeptide composition as revealed by analysis of mutants. J Cell Biol* ***91:****69-76.*
2. ***Afzelius, B. A.*** *2004. Cilia-related diseases. J Pathol* ***204:****470-7.*
3. ***Avidor-Reiss, T., A. M. Maer, E. Koundakjian, A. Polyanovsky, T. Keil, et al.*** *2004. Decoding cilia function: defining specialized genes required for compartmentalized cilia biogenesis. Cell* ***117:****527-39.*
4. ***Bastin, P., K. Ellis, L. Kohl, and K. Gull.*** *2000. Flagellum ontogeny in trypanosomes studied via an inherited and regulated RNA interference system. J Cell Sci* ***113:****3321-3328.*
5. ***Bastin, P., K. R. Matthews, and K. Gull.*** *1996. The paraflagellar rod of Kinetoplastida: solved and unsolved questions. Parasitol. Today* ***12:****302-307.*
6. ***Bastin, P., T. J. Pullen, T. Sherwin, and K. Gull.*** *1999. Protein transport and flagellum assembly dynamics revealed by analysis of the paralysed trypanosome mutant snl-1. J. Cell Sci.* ***112:****3769-77.*
7. ***Bastin, P., T. Sherwin, and K. Gull.*** *1998. Paraflagellar rod is vital for trypanosome motility. Nature* ***391:****548.*
8. ***Brown, J. M., C. Hardin, and J. Gaertig.*** *1999. Rotokinesis, a novel phenomenon of cell locomotion-assisted cytokinesis in the ciliate Tetrahymena thermophila. Cell Biol Int* ***23:****841-8.*
9. ***Cachon, J., M. Cachon, M.-P. Cosson, and C. J.*** *1988. The paraflagellar rod: a structure in search of a function. Biol. Cell* ***63:****169-181.*
10. ***Chu, D. T., and M. W. Klymkowsky.*** *1989. The appearance of acetylated alpha-tubulin during early development and cellular differentiation in Xenopus. Dev Biol* ***136:****104-17.*
11. ***Cosson, J.*** *1996. A moving image of flagella: news and views on the mechanisms involved in axonemal beating. Cell. Biol. Int.* ***20:****83-94.*
12. ***Curry, A. M., and J. L. Rosenbaum.*** *1993. Flagellar radial spoke: a model molecular genetic system for studying organelle assembly. Cell Motil Cytoskeleton* ***24:****224-32.*
13. ***Diener, D. R., L. H. Ang, and J. L. Rosenbaum.*** *1993. Assembly of flagellar radial spoke proteins in Chlamydomonas: identification of the axoneme binding domain of radial spoke protein 3. J Cell Biol* ***123:****183-90.*
14. ***Durand-Dubief, M., L. Kohl, and P. Bastin.*** *2003. Efficiency and specificity of RNA interference generated by intra- and intermolecular double stranded RNA in Trypanosoma brucei. Mol Biochem Parasitol* ***129:****11-21.*
15. ***Dutcher, S. K., B. Huang, and D. J. Luck.*** *1984. Genetic dissection of the central pair microtubules of the flagella of Chlamydomonas reinhardtii. J Cell Biol* ***98:****229-36.*
16. ***Gardner, L. C., E. O'Toole, C. A. Perrone, T. Giddings, and M. E. Porter.*** *1994. Components of a "dynein regulatory complex" are located at the junction between the radial spokes and the dynein arms in Chlamydomonas flagella. J Cell Biol* ***127:****1311-25.*
17. ***Gull, K.*** *1999. The cytoskeleton of trypanosomatid parasites. Annu. Rev. Microbiol.* ***53:****629-55.*
18. ***Hill, K. L.*** *2003. Mechanism and biology of trypanosome cell motility. Euk Cell* ***2:****200-8.*
19. ***Hill, K. L., N. R. Hutchings, P. M. Grandgenett, and J. E. Donelson.*** *2000. T Lymphocyte triggering factor of African trypanosomes is associated with the flagellar*

fraction of the cytoskeleton and represents a new family of proteins that are present in several divergent eukaryotes. J. Biol. Chem. ***275:****39369–39378.*

20. ***Hill, K. L., N. R. Hutchings, D. G. Russell, and J. E. Donelson.*** *1999. A novel protein targeting domain directs proteins to the anterior cytoplasmic face of the flagellar pocket in African trypanosomes. J. Cell Sci.* ***112:****3091-101.*
21. ***Hill, K. L., H. H. Li, J. Singer, and S. Merchant.*** *1991. Isolation and structural characterization of the Chlamydomonas reinhardtii gene for cytochrome c6. Analysis of the kinetics and metal specificity of its copper-responsive expression. J Biol Chem* ***266:****15060-7.*
22. ***Holwill, M. E.*** *1974. Some physical aspects of the motility of ciliated and flagellated microorganisms. Sci Prog* ***61:****63-80.*
23. ***Holwill, M. E. J.*** *1965. The Motion of Strigomona Oncopelti. J. Exp. Biol.* ***42:****125-137.*
24. ***Huang, B., Z. Ramanis, and D. J. Luck.*** *1982. Suppressor mutations in Chlamydomonas reveal a regulatory mechanism for Flagellar function. Cell* ***28:****115-24.*
25. ***Hungerglaser, I., and T. Seebeck.*** *1997. Deletion of the genes for the paraflagellar rod protein PFR-A In Trypanosoma brucei Is Probably Lethal. Molecular and Biochemical Parasitology* ***90:****347-351.*
26. ***Hutchings, N. R., J. E. Donelson, and K. L. Hill.*** *2002. Trypanin is a cytoskeletal linker protein and is required for cell motility in African trypanosomes. Journal of Cell Biology* ***156:****867-877.*
27. ***Ibanez-Tallon, I., N. Heintz, and H. Omran.*** *2003. To beat or not to beat: roles of cilia in development and disease. Hum Mol Genet* ***12 Spec No 1:****R27-35.*
28. ***Kohl, L., D. Robinson, and P. Bastin.*** *2003. Novel roles for the flagellum in cell morphogenesis and cytokinesis of trypanosomes. Embo J* ***22:****5336-46.*
29. ***Kohl, L., T. Sherwin, and K. Gull.*** *1999. Assembly of the paraflagellar rod and the flagellum attachment zone complex during the Trypanosoma brucei cell cycle. J Eukaryot Microbiol* ***46:****105-109.*
30. ***LaCount, D. J., B. Barrett, and J. E. Donelson.*** *2002. Trypanosoma brucei FLA1 is required for flagellum attachment and cytokinesis. J Biol Chem* ***277:****17580-8.*
31. ***Li, J. B., J. M. Gerdes, C. J. Haycraft, Y. Fan, T. M. Teslovich, et al.*** *2004. Comparative genomics identifies a flagellar and basal body proteome that includes the BBS5 human disease gene. Cell* ***117:****541-52.*
32. ***Lindemann, C. B., and K. S. Kanous.*** *1997. A model for flagellar motility. Int. Rev. Cytol.* ***173:****1-72.*
33. ***Manson, M. D., J. P. Armitage, J. A. Hoch, and R. M. Macnab.*** *1998. Bacterial locomotion and signal transduction. J Bacteriol* ***180:****1009-22.*
34. ***Mastronarde, D. N., E. T. O'Toole, K. L. McDonald, J. R. McIntosh, and M. E. Porter.*** *1992. Arrangement of inner dynein arms in wild-type and mutant flagella of Chlamydomonas. J Cell Biol* ***118:****1145-62.*
35. ***McKean, P. G., A. Baines, S. Vaughan, and K. Gull.*** *2003. Gamma-tubulin functions in the nucleation of a discrete subset of microtubules in the eukaryotic flagellum. Curr Biol* ***13:****598-602.*
36. ***Mitchell, D. R.*** *2000. Chlamydomonas Flagella. J. of Phycol.* ***36:****261-273.*
37. ***Moreira-Leite, F. F., T. Sherwin, L. Kohl, and K. Gull.*** *2001. A trypanosome structure involved in transmitting cytoplasmic information during cell division. Science* ***294:****610-2.*

38. **Ngo, H., C. Tschudi, K. Gull, and E. Ullu.** *1998. Double-stranded RNA induces mRNA degradation in Trypanosoma brucei. Proc Natl Acad Sci U S A* ***95:****14687-92.*
39. **Ogbadoyi, E. O., D. R. Robinson, and K. Gull.** *2003. A high-order trans-membrane structural linkage is responsible for mitochondrial genome positioning and segregation by flagellar basal bodies in trypanosomes. Mol Biol Cell* ***14:****1769-79.*
40. **Omoto, C. K., I. R. Gibbons, R. Kamiya, C. Shingyoji, K. Takahashi, et al.** *1999. Rotation of the central pair microtubules in eukaryotic flagella. Mol Biol Cell* ***10:****1-4.*
41. **Omoto, C. K., T. Yagi, E. Kurimoto, and R. Kamiya.** *1996. Ability of paralyzed flagella mutants of Chlamydomonas to move. Cell Motil Cytoskeleton* ***33:****88-94.*
42. **Pepin, J., and J. E. Donelson.** *1999. African trypanosomiasis (Sleeping Sickness), p. 774 - 784. In R. Guerrant, D. H. Walker, and P. F. Weller (ed.), Tropical Infectious Diseases: Principles, Pathogens and Practice., 1st ed, vol. 1. Churchill Livingstone, Philadelphia, PA.*
43. **Piperno, G., K. Mead, M. LeDizet, and A. Moscatelli.** *1994. Mutations in the "dynein regulatory complex" alter the ATP-insensitive binding sites for inner arm dyneins in Chlamydomonas axonemes. J Cell Biol* ***125:****1109-17.*
44. **Piperno, G., K. Mead, and W. Shestak.** *1992. The inner dynein arms I2 interact with a "dynein regulatory complex" in Chlamydomonas flagella. J Cell Biol* ***118:****1455-63.*
45. **Poltera, A. A.** *1985. Pathology of human African trypanosomiasis with reference to experimental African trypanosomiasis and infections of the central nervous system. Br Med Bull* ***41:****169-74.*
46. **Porter, M. E., J. A. Knott, L. C. Gardner, D. R. Mitchell, and S. K. Dutcher.** *1994. Mutations in the SUP-PF-1 locus of Chlamydomonas reinhardtii identify a regulatory domain in the beta-dynein heavy chain. J Cell Biol* ***126:****1495-507.*
47. **Porter, M. E., J. Power, and S. K. Dutcher.** *1992. Extragenic suppressors of paralyzed flagellar mutations in Chlamydomonas reinhardtii identify loci that alter the inner dynein arms. J Cell Biol* ***118:****1163-76.*
48. **Porter, M. E., and W. S. Sale.** *2000. The 9 + 2 axoneme anchors multiple inner arm dyneins and a network of kinases and phosphatases that control motility. J Cell Biol* ***151:****F37-42.*
49. **Redmond, S., J. Vadivelu, and M. C. Field.** *2003. RNAit: an automated web-based tool for the selection of RNAi targets in Trypanosoma brucei. Mol Biochem Parasitol* ***128:****115-8.*
50. **Reichl, E. M., J. C. Effler, and D. N. Robinson.** *2005. The stress and strain of cytokinesis. Trends Cell Biol* ***15:****200-6.*
51. **Robinson, D., P. Beattie, T. Sherwin, and K. Gull.** *1991. Microtubules, tubulin, and microtubule-associated proteins of trypanosomes. Methods. Enzymol.* ***196:****285-99.*
52. **Robinson, D. R., and K. Gull.** *1991. Basal body movements as a mechanism for mitochondrial genome segregation in the trypanosome cell cycle. Nature* ***352:****731-3.*
53. **Robinson, D. R., T. Sherwin, A. Ploubidou, E. H. Byard, and K. Gull.** *1995. Microtubule polarity and dynamics in the control of organelle positioning, segregation, and cytokinesis in the trypanosome cell cycle. Journal of Cell Biology* ***128:****1163-72.*
54. **Rupp, G., E. O'Toole, L. C. Gardner, B. F. Mitchell, and M. E. Porter.** *1996. The sup-pf-2 mutations of Chlamydomonas alter the activity of the outer dynein arms by modification of the gamma-dynein heavy chain. J Cell Biol* ***135:****1853-65.*

55. ***Rupp, G., and M. E. Porter.*** *2003. A subunit of the dynein regulatory complex in Chlamydomonas is a homologue of a growth arrest-specific gene product. J Cell Biol* ***162:****47-57.*

56. ***Sapiro, R., I. Kostetskii, P. Olds-Clarke, G. L. Gerton, G. L. Radice, et al.*** *2002. Male infertility, impaired sperm motility, and hydrocephalus in mice deficient in sperm-associated antigen 6. Mol Cell Biol* ***22:****6298-305.*

57. ***Satir, P.*** *1995. Landmarks in cilia research from Leeuwenhoek to us. Cell Motil. Cytoskel.* ***32:****90-4.*

58. ***Sherwin, T., and K. Gull.*** *1989. The cell division cycle of Trypanosoma brucei brucei: timing of event markers and cytoskeletal modulations. Philos. Trans. R. Soc. Lond. Ser. B, Biol. Sci.* ***323:****573-88.*

59. ***Smith, E. F., and P. A. Lefebvre.*** *1996. PF16 encodes a protein with armadillo repeats and localizes to a single microtubule of the central apparatus in Chlamydomonas flagella. J Cell Biol* ***132:****359-70.*

60. ***Smith, E. F., and P. A. Lefebvre.*** *1997. PF20 gene product contains WD repeats and localizes to the intermicrotubule bridges in Chlamydomonas flagella. Mol Biol Cell* ***8:****455-67.*

61. ***Smith, E. F., and W. S. Sale.*** *1992. Regulation of dynein-driven microtubule sliding by the radial spokes in flagella. Science* ***257:****1557-9.*

62. ***Smith, E. F., and P. Yang.*** *2004. The radial spokes and central apparatus: mechano-chemical transducers that regulate flagellar motility. Cell Motil Cytoskeleton* ***57:****8-17.*

63. ***Snell, W. J., J. Pan, and Q. Wang.*** *2004. Cilia and flagella revealed: from flagellar assembly in Chlamydomonas to human obesity disorders. Cell* ***117:****693-7.*

64. ***Sugrue, P., M. R. Hirons, J. U. Adam, and M. E. Holwill.*** *1988. Flagellar wave reversal in the kinetoplastid flagellate Crithidia oncopelti. Biol Cell* ***63:****127-31.*

65. ***Thompson, J. D., D. G. Higgins, and T. J. Gibson.*** *1994. CLUSTAL W: improving the sensitivity of progressive multiple sequence alignment through sequence weighting, position-specific gap penalties and weight matrix choice. Nucleic Acids Res* ***22:****4673-80.*

66. ***Van Den Abbeele, J., Y. Claes, D. van Bockstaele, D. Le Ray, and M. Coosemans.*** *1999. Trypanosoma brucei spp. development in the tsetse fly: characterization of the post-mesocyclic stages in the foregut and proboscis. Parasitology* ***118:****469-78.*

67. ***Vickerman, K.*** *1969. On the surface coat and flagellar adhesion in trypanosomes. J Cell Sci* ***5:****163-93.*

68. ***Vickerman, K., L. Tetley, K. A. Hendry, and C. M. Turner.*** *1988. Biology of African trypanosomes in the tsetse fly. Biol Cell* ***64:****109-19.*

69. ***Walker, P. J.*** *1961. Organization of function in trypanosome flagella. Nature* ***189:****1017-1018.*

70. ***Walker, P. J., and J. C. Walker.*** *1963. Movement of trypanosome flagella. J. of Protozoology* ***10, suppl:****32.*

71. ***Wargo, M. J., M. A. McPeek, and E. F. Smith.*** *2004. Analysis of microtubule sliding patterns in Chlamydomonas flagellar axonemes reveals dynein activity on specific doublet microtubules. J Cell Sci* ***117:****2533-44.*

72. ***Wargo, M. J., and E. F. Smith.*** *2003. Asymmetry of the central apparatus defines the location of active microtubule sliding in Chlamydomonas flagella. Proc Natl Acad Sci U S A* ***100:****137-42.*

73. ***Williams, B. D., M. A. Velleca, A. M. Curry, and J. L. Rosenbaum.*** *1989. Molecular cloning and sequence analysis of the Chlamydomonas gene coding for radial spoke protein 3: flagellar mutation pf-14 is an ochre allele. J Cell Biol* ***109:****235-45.*

74. ***Wirtz, E., S. Leal, C. Ochatt, and G. A. Cross.*** *1999. A tightly regulated inducible expression system for conditional gene knock-outs and dominant-negative genetics in Trypanosoma brucei. Mol. Biochem. Parasitol.* ***99:****89-101.*

75. ***Yang, P., D. R. Diener, J. L. Rosenbaum, and W. S. Sale.*** *2001. Localization of calmodulin and dynein light chain LC8 in flagellar radial spokes. J Cell Biol* ***153:****1315-26.*

76. ***Zhang, Z., I. Kostetskii, S. B. Moss, B. H. Jones, C. Ho, et al.*** *2004. Haploinsufficiency for the murine orthologue of Chlamydomonas PF20 disrupts spermatogenesis. Proc Natl Acad Sci U S A* ***101:****12946-51.*

77. ***Zhang, Z., R. Sapiro, D. Kapfhamer, M. Bucan, J. Bray, et al.*** *2002. A sperm-associated WD repeat protein orthologous to Chlamydomonas PF20 associates with Spag6, the mammalian orthologue of Chlamydomonas PF16. Mol Cell Biol* ***22:****7993-8004.*

FIGURE LEGENDS

Figure 1. RSP3, PF16 and PF20 protein alignments. Alignments of full-length RSP3 (A), PF16 (B) and PF20 (C) proteins from *Homo sapiens* (Hs), *C. reinhardtii* (Cr), *T. brucei* (Tb), *T. cruzi* (Tc) and *Leishmania major* (Lm) are shown. Residues that are conserved in all four proteins are shaded yellow, while residues that are conserved in three or more proteins are shaded blue and conservative substitutions are shaded green.

Figure 2. RSP3, PF16 and PF20 are required for flagellar motility. (A) Northern blot demonstrating efficient RNAi knockdown of each target. TbRSP3, TbPF16 and TbPF20 cells were incubated in the presence (+) or absence (-) of tetracycline (Tet). Total RNA was prepared 24 hours after the addition of tetracycline and subjected to Northern blot analysis using RSP3, PF16 or PF20 probes as indicated. The lower blots show loading controls. (B) Sedimentation assay demonstrating that *rsp3, pf16* and *pf20* mutants have abnormal motility. TbRSP3, TbPF16 and TbPF20 cells were incubated in the presence (open symbols) or absence (filled symbols) of tetracycline for 24 hours and assayed for sedimentation as described in Materials and Methods. Sedimentation curves represent averages of two independent experiments and error bars reflect standard deviation. *(C) Representative transmission electron micrographs of axonemes from TbRSP3 cells incubated with (+ Tet) or without (- Tet) tetracycline. Arrows point out an example of a spoke in the – Tet sample and the equivalent position in the + Tet sample, where the spoke is absent.* (D) Radial spokes are reduced but not completely absent in *rsp3* mutant axonemes. The number of spokes in EM sections of TbRSP3 cells incubated with or without tetracycline was determined. The percent of sections having 0 – 9 spokes are shown.

Figure 3. Orientation of the central pair is variable in *pf16* and *pf20* mutants. (A and B) Representative EM images of flagella from TbPF16 cells grown in the absence (A, control) or presence (B, + Tet) of tetracycline. In control cells (A), the central pair microtubules lie in a plane that is roughly parallel to the PFR, while in *pf16* knockdown mutants (B) central pair orientation is variable. Scalebar is 100 nm. (C) Central pair orientation was measured (Materials and Methods) in *pf20* control cells (n = 19), pf20 mutants (+ Tet, n = 18), *pf16* control cells (n = 26) and *pf16* mutants (+ Tet, n = 26). For illustration purposes, the line bisecting C1 and C2 in each sample is depicted within a schematic diagram of the 9 + 2 axoneme at the top of the chart.

Figure 4. *rsp3* mutants are defective in cytokinesis. (A) DIC images of live *rsp3* mutants in multicellular clusters 48 hours after the addition of tetracycline (each image is a frame taken from Supplemental Videos 6 - 7). Small clusters of a few cells are observed within 24 hours post-induction and by 4 – 5 days post-induction, the majority of cells are found in massive clusters, ***e.g.*** see figure 6B. Data are shown for *rsp3* mutants and the same phenotype is seen in *pf16* and *pf20* mutants (not shown). Arrows denote the posterior ends of cell bodies conjoined in clusters. (B) Motility mutants are blocked in the completion of cytokinesis. TbRSP3 cells incubated in the presence (+Tet, n = 792) or absence (-Tet, n =676) of drug were examined by phase-contrast microscopy 48 hours after the addition of tetracycline. Cells were classified as described in the text. The percentage of cells in each category is indicated. In this experiment, two replicates were quantified (+Tet, n = 393 and n = 399; -Tet, n = 334 and n =342), with standard deviation indicated. These data are representative of three independent experiments.

Figure 5. *pfr2* mutants are defective in cytokinesis. (A) Northern blot demonstrating efficient RNAi knockdown of PFR2 in two independent knockdown cell lines. TbPFR2-1 (RNAi Target 1) and TbPFR2-2 (RNAi Target 2) cells were incubated in the presence (+) or absence (-) of tetracycline (Tet). Total RNA was prepared 24 hours after the addition of tetracycline and subjected to Northern blot analysis using a PFR2 probe as indicated. The lower blot shows a loading control. (B) Western blot analysis of whole cell lysates from TbPFR2-1 and TbPFR2-2 cells incubated in the presence (+) or absence (-) of tetracycline (Tet). Protein samples were prepared 24 and 48 hours after the addition of tetracycline and subjected to Western blot analysis with an α-PFR2 monoclonal antibody (upper panel) or an α-β-Tubulin monoclonal antibody as a loading control (lower panel). (C) DIC images of live *pfr2* mutants in multicellular clusters 48 hours after the addition of tetracycline. TbPFR2-1 cells (left panel) and TbPFR2-2 cells (right panel) are shown. Arrows denote the posterior ends of cell bodies conjoined in clusters (each image is a frame taken from Supplemental Videos 9 - 10). (D) By four days post-induction, the majority of cells are found in massive multicellular clusters. Phase-contrast images of live cultures incubated with (+Tet) or *without (-Tet)* tetracycline are shown at 20X magnification (upper panels) and 10X magnification (lower panels). Images shown are from TbPFR2-1 cultures. Massive clusters are similarly observed in TbPFR2-2 cultures. (E) Growth curves of TbPFR2-1 cells grown in the presence (open symbols) or absence (filled symbols) of tetracycline, where tetracycline was added at time = 0.

Figure 6. Physical agitation of motility mutants rescues the cytokinesis defect. (A) Growth curves of TbRSP3 cells grown on a rotating shaker (triangles) or grown without shaking (circles), in the presence (open symbols) or absence (filled symbols) of tetracycline, where

tetracycline was added at time = 0. (B) Phase contrast images of live tetracycline-induced TbRSP3 cultures, 66 hours post-induction. Cultures grown without shaking are shown in the left panels, while cultures grown with shaking are shown in the right panels. Images are shown at 20X (upper panels) and 10X (lower panels) magnification. Rotating also rescued the cytokinesis defect of *pf16* and *pf20* mutants (not shown).

Figure 7. *rsp3/tpn* and *pf16/tpn* double knockdown mutants. (A, B) Northern blots demonstrating efficient RNAi knockdown of TPN, RSP3, and PF16 in single and double knockdown mutants. RNAi targets are indicated for each cell line, TbRSP3 (RSP3), TbTPN (TPN), TbPF16 (PF16), TbRSP3/TPN (RSP3/TPN), and TbPF16/TPN (PF16/TPN). Cells were incubated in the presence (+) or absence (-) of tetracycline (Tet) for 24 hours and total RNA was isolated and subjected to Northern blot analysis with TPN, RSP3, or PF16 probes, as indicated. The lower blots show loading controls. (C) Western blot analysis of whole cell lysates from TbPF16/TPN (PF16/TPN), TbRSP3/TPN (RSP3/TPN), and TbTPN (TPN) cells incubated in the presence (+) or absence (-) of tetracycline (Tet). Protein samples were prepared 24 and 48 hours after the addition of tetracycline and subjected to Western blot analysis with an α-TPN monoclonal antibody (upper panel) or an α-β-Tubulin monoclonal antibody as a loading control (lower panel).

Figure 8. Loss of trypanin suppresses the flagellar beat defect of a central pair mutant. Images show a time-lapse series of *pf16* single mutants (A) and *pf16/tpn* double mutants (B), taken every 1/6 of a second over a one second time period. All cells are shown with their anterior ends oriented downward, with arrows indicating the position of the flagellar tip. The hallmark of

pf16 single mutants is an S-shaped curvature of the anterior portion of the cell body and flagellar tip, accompanied by an abnormal flagellar beat (see text and Supplemental Video 3). *pf16/tpn* double mutants do not typically exhibit this anterior curvature and sustain a more normal flagellar beat (compare Supplemental Videos 11 and 12 with Video 3). (C) Quantitative analysis of flagellar beating in *pf16* single mutant and *pf16/tpn* double mutant cultures. 100 random cells from each cell line were analyzed 48 hours after the addition of tetracycline. The number of beats at the flagellar tip, up to 12 or greater than 12 (>12), during a 10 second period were quantified for each cell. Overall cellular movements in this time period were also analyzed and cells that exhibited no net movement (Immotile) or net movement (Motile) are indicated. Note that while this quantitative assay clearly demonstrates suppression of *pf16* defects, it does not reflect the improved quality of beat in the double mutant. For example, although some *pf16* and *pf16/tpn* mutants fall into the same ">12" quantitative category, there are obvious qualitative differences in flagellar motion between these mutants (e.g. compare Supplemental Videos 11 and 12 with Video 4).

Figure 1

A

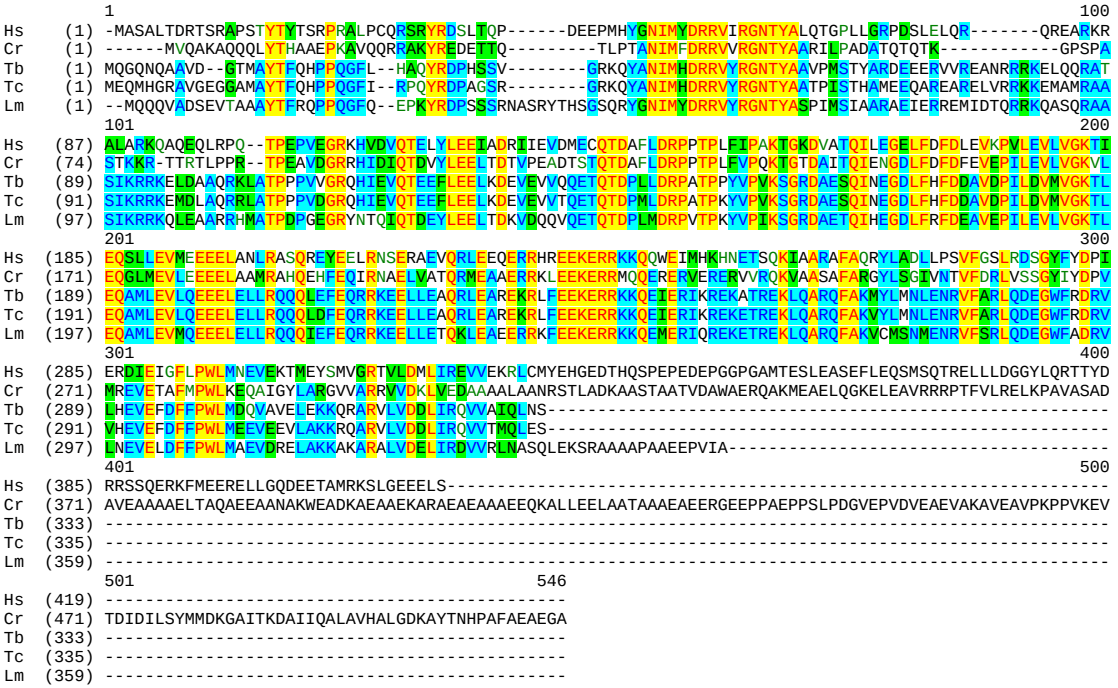

B

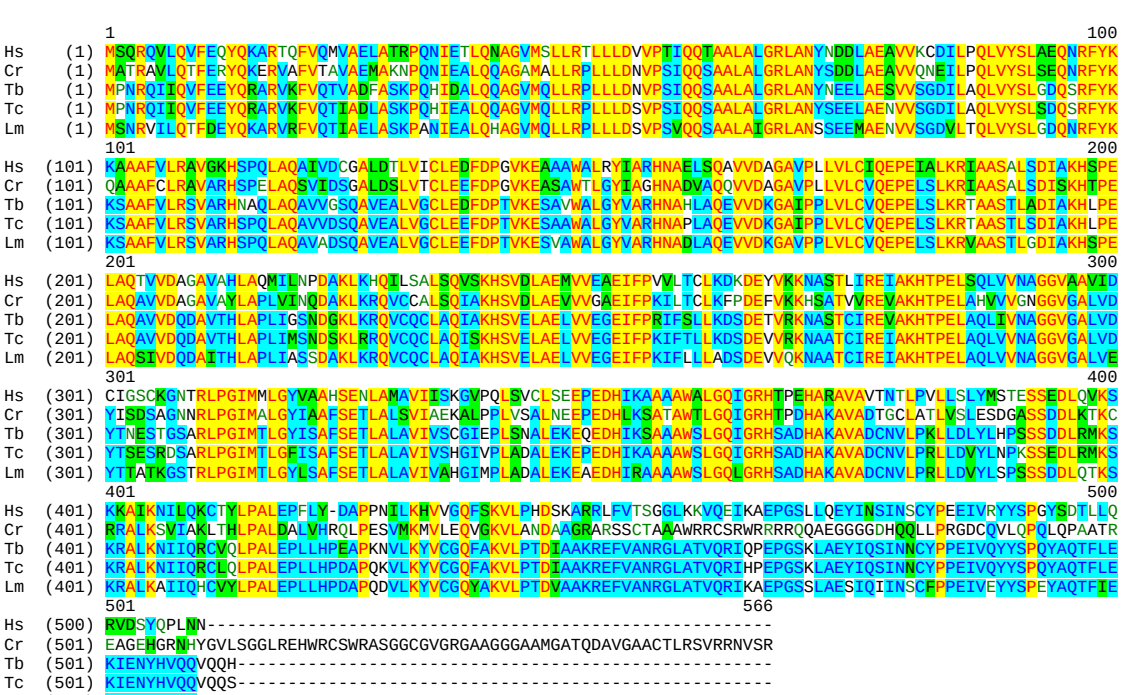

Figure 1, contd.

C

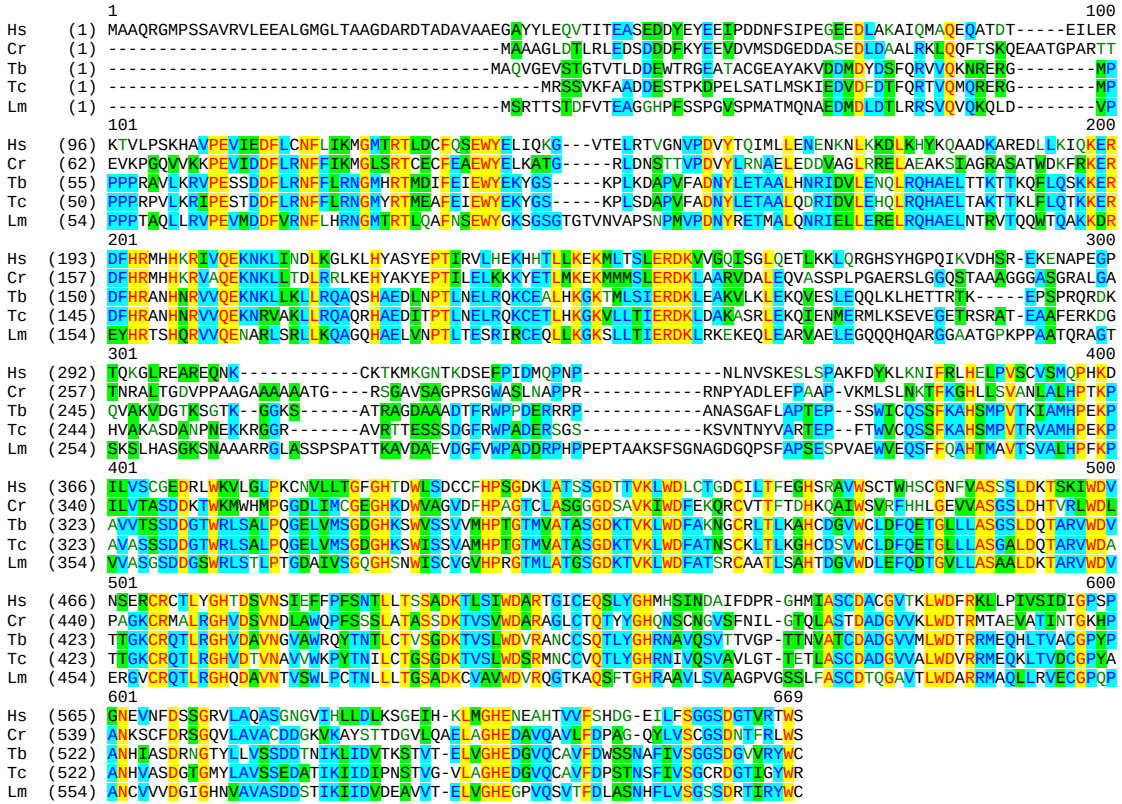

Figure 2

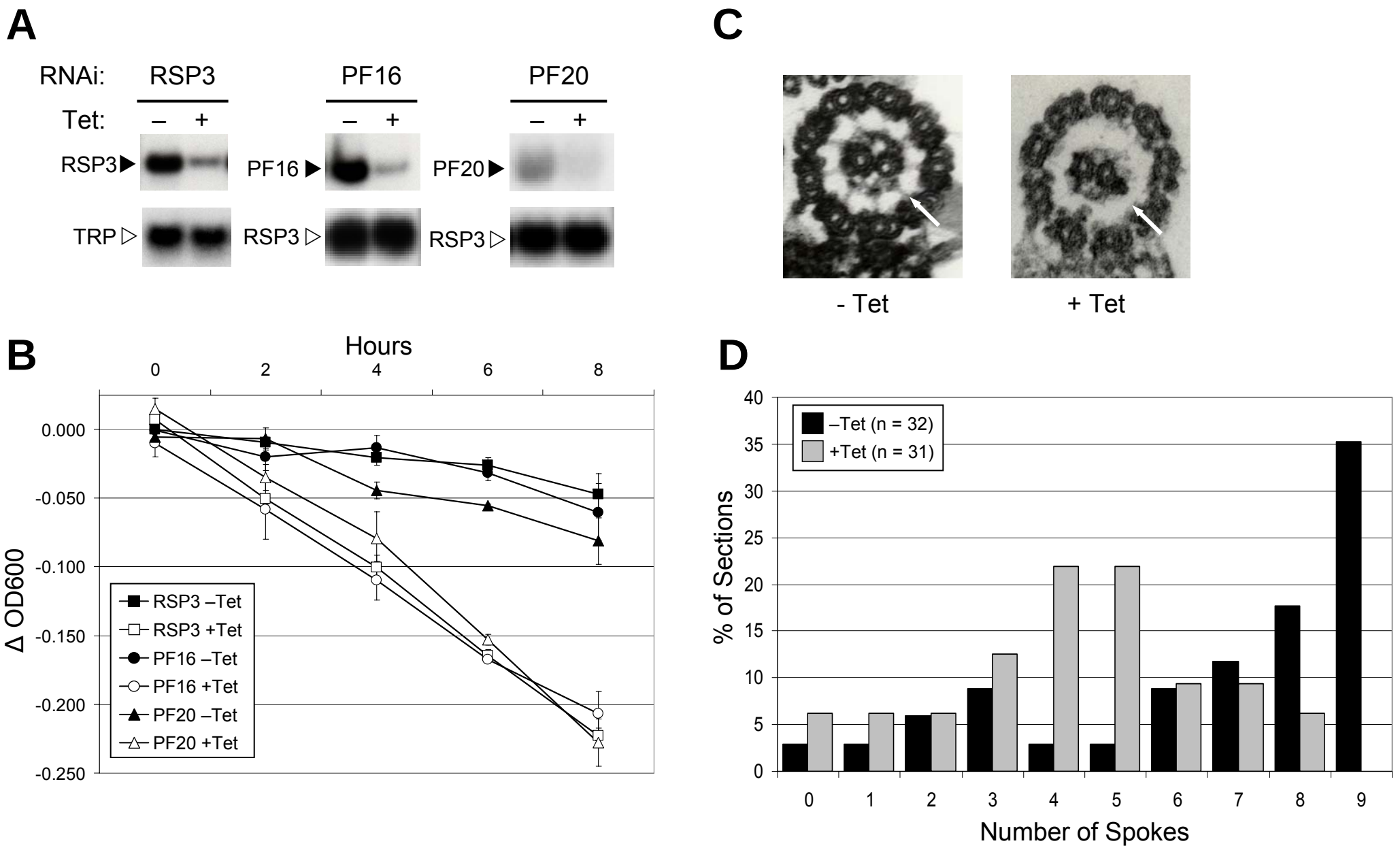
A
RNAi:
RSP3
PF16
PF20
Tet:
– +
– +
– +
RSP3▶
PF16▶
PF20▶
TRP▷
RSP3▷
RSP3▷
C
- Tet
+ Tet
B
Hours
0
2
4
6
8
0.000
-0.050
-0.100
-0.150
-0.200
-0.250
Δ OD600
RSP3 –Tet
RSP3 +Tet
PF16 –Tet
PF16 +Tet
PF20 –Tet
PF20 +Tet
D
40
35
30
25
20
15
10
5
0
% of Sections
–Tet (n = 32)
+Tet (n = 31)
0
1
2
3
4
5
6
7
8
9
Number of Spokes

Figure 3

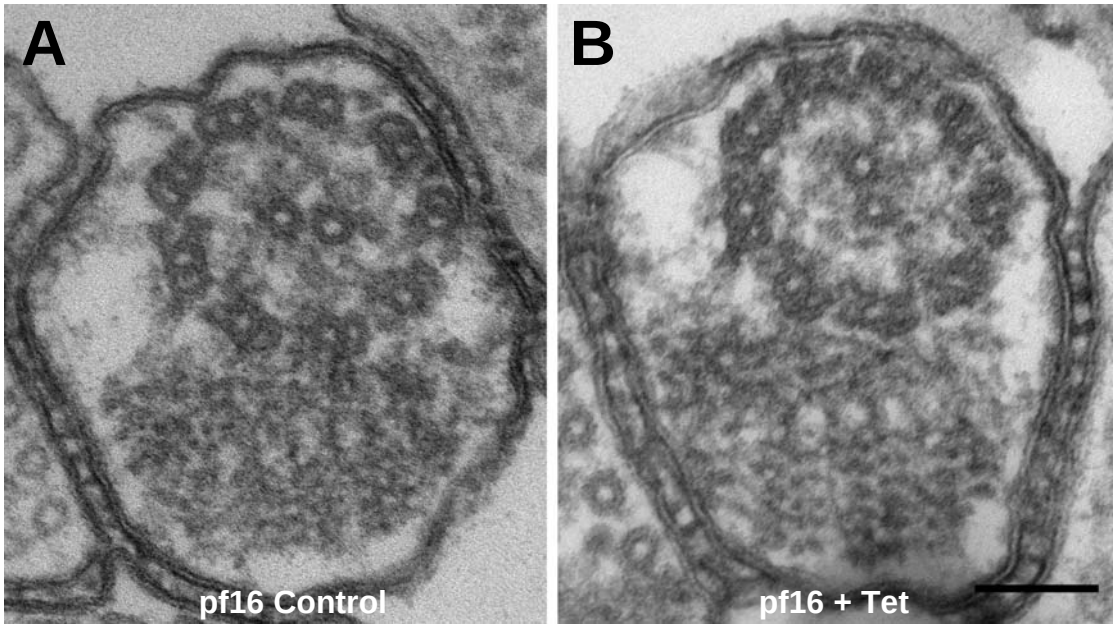
A
pf16 Control
B
pf16 + Tet

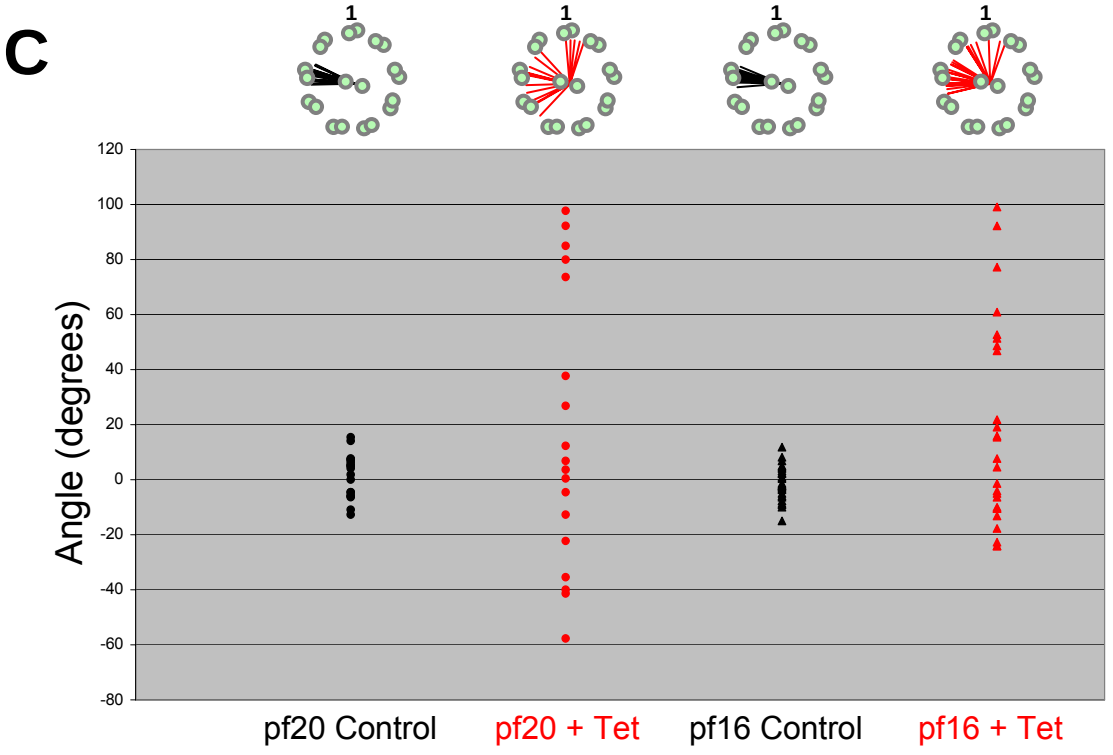
C
1
1
1
1
120
100
80
60
40
20
0
-20
-40
-60
-80
Angle (degrees)
pf20 Control
pf20 + Tet
pf16 Control
pf16 + Tet

Figure 4

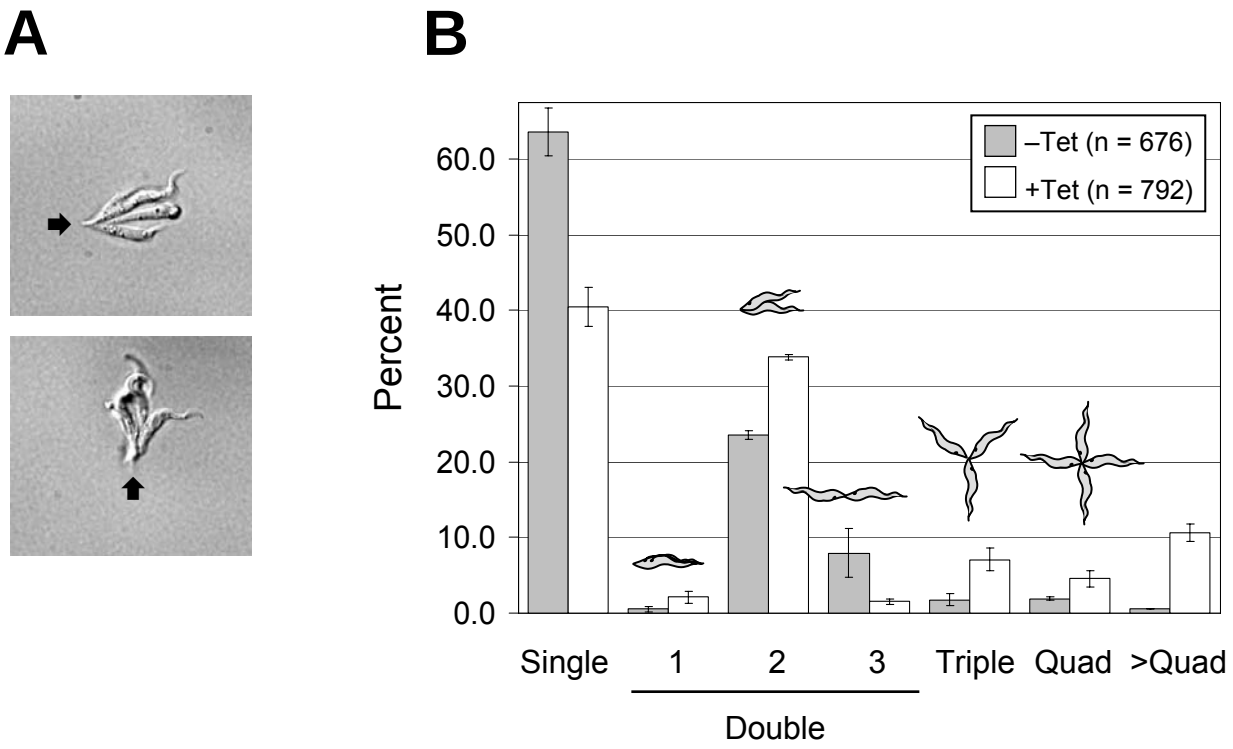
A
B
–Tet (n = 676)
+Tet (n = 792)
Percent
60.0
50.0
40.0
30.0
20.0
10.0
0.0
Single
1
2
3
Triple
Quad
>Quad
Double

Figure 5

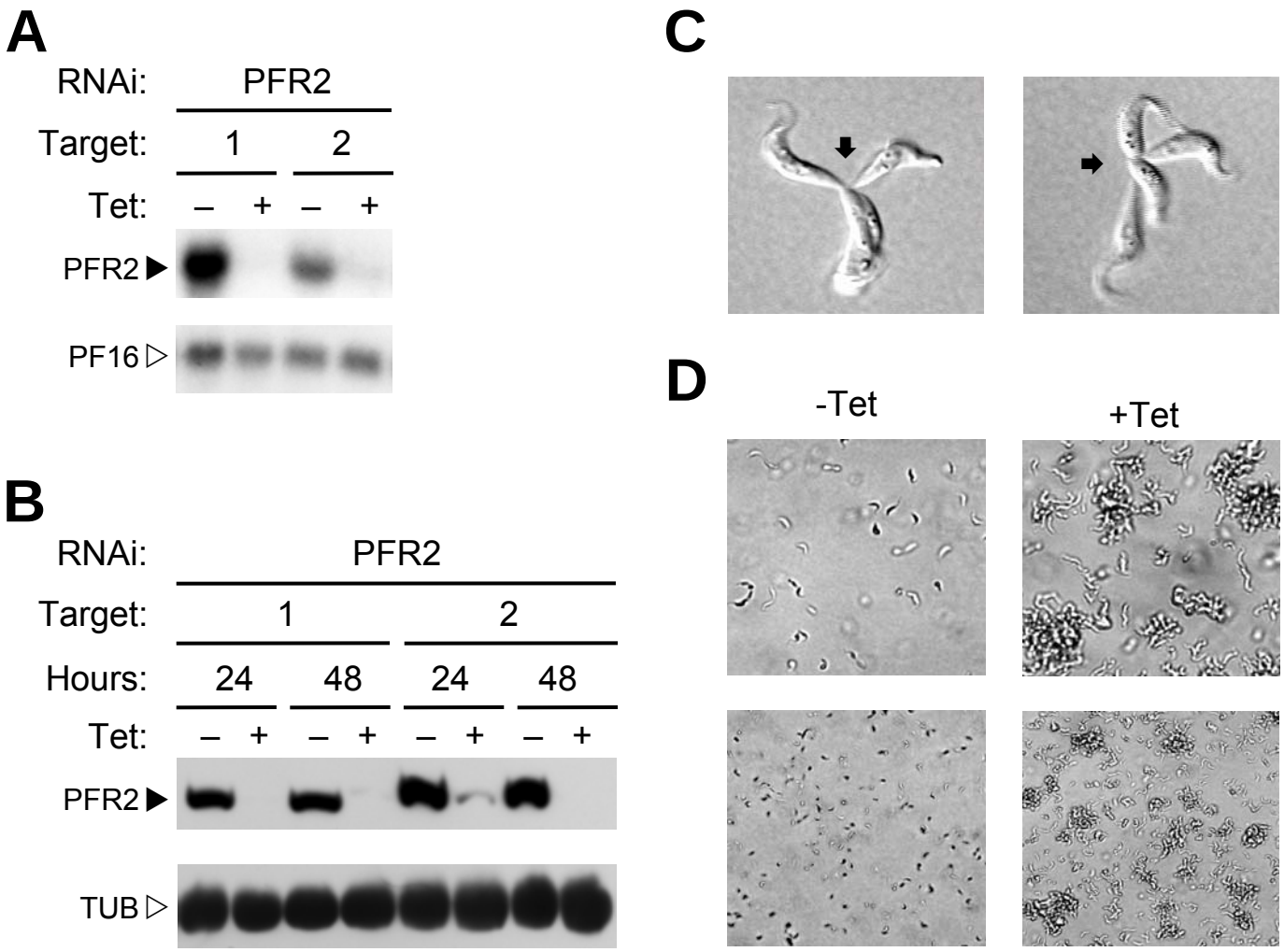
A
RNAi:
PFR2
Target:
1
2
Tet:
– + – +
PFR2▶
PF16▷
B
RNAi:
PFR2
Target:
1
2
Hours:
24
48
24
48
Tet:
– + – + – + – +
PFR2▶
TUB▷
C
D
-Tet
+Tet

Figure 5, contd.

E

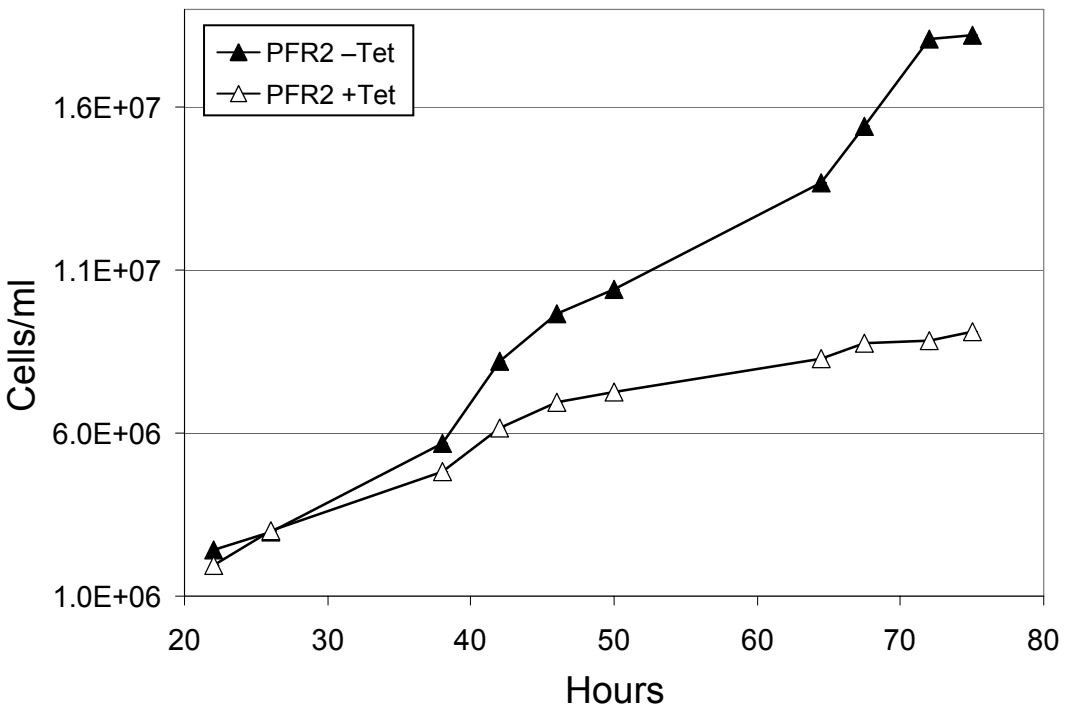

Figure 6

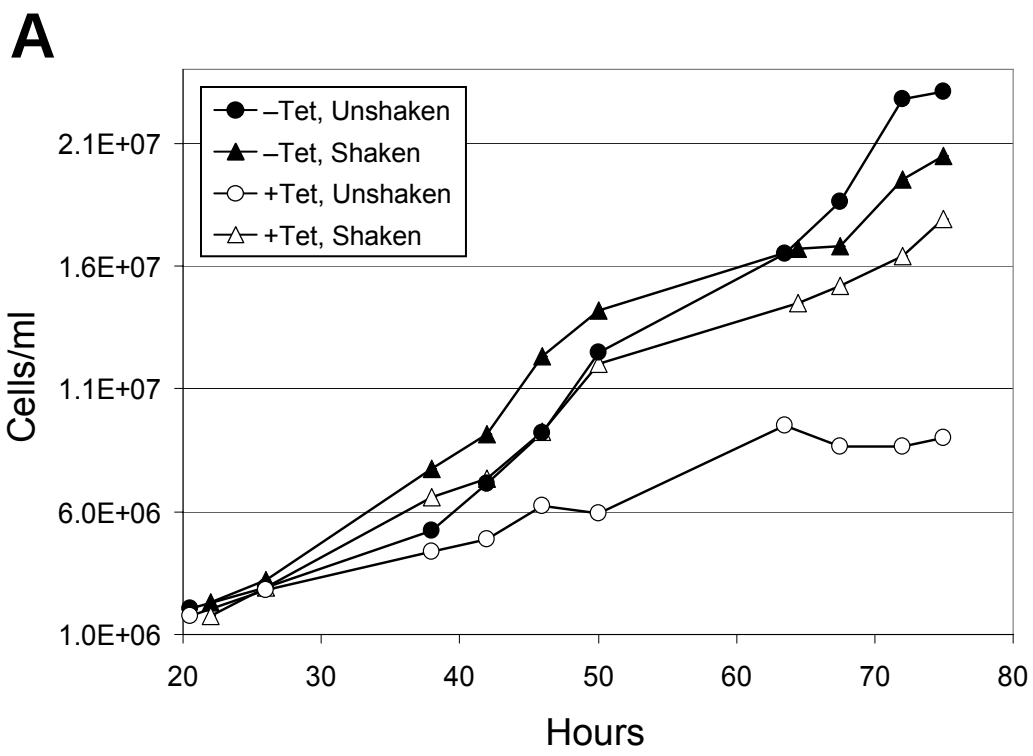
A
–Tet, Unshaken
–Tet, Shaken
+Tet, Unshaken
+Tet, Shaken
2.1E+07
1.6E+07
1.1E+07
6.0E+06
1.0E+06
Cells/ml
20
30
40
50
60
70
80
Hours

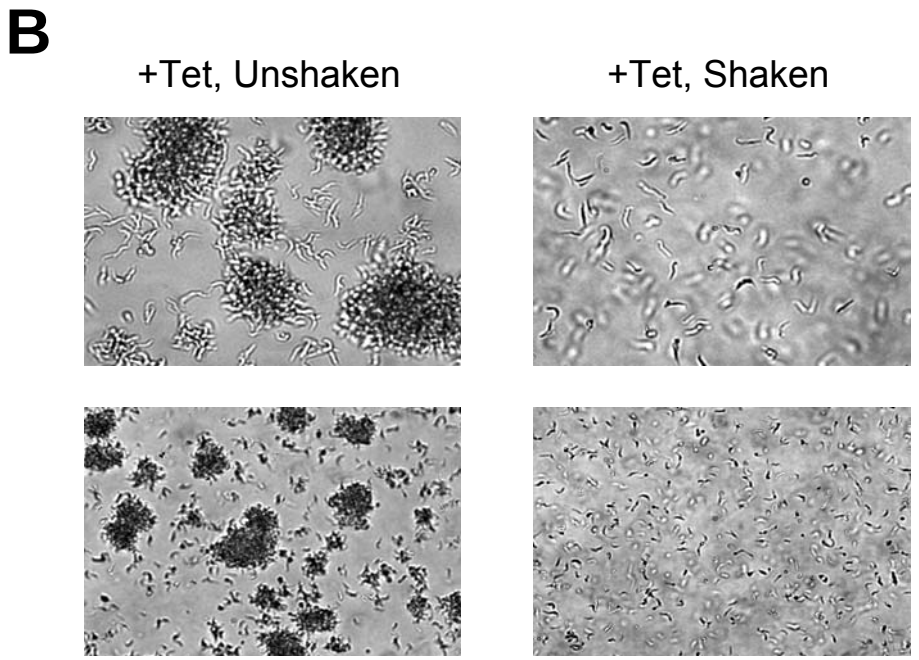
B
+Tet, Unshaken
+Tet, Shaken

Figure 7

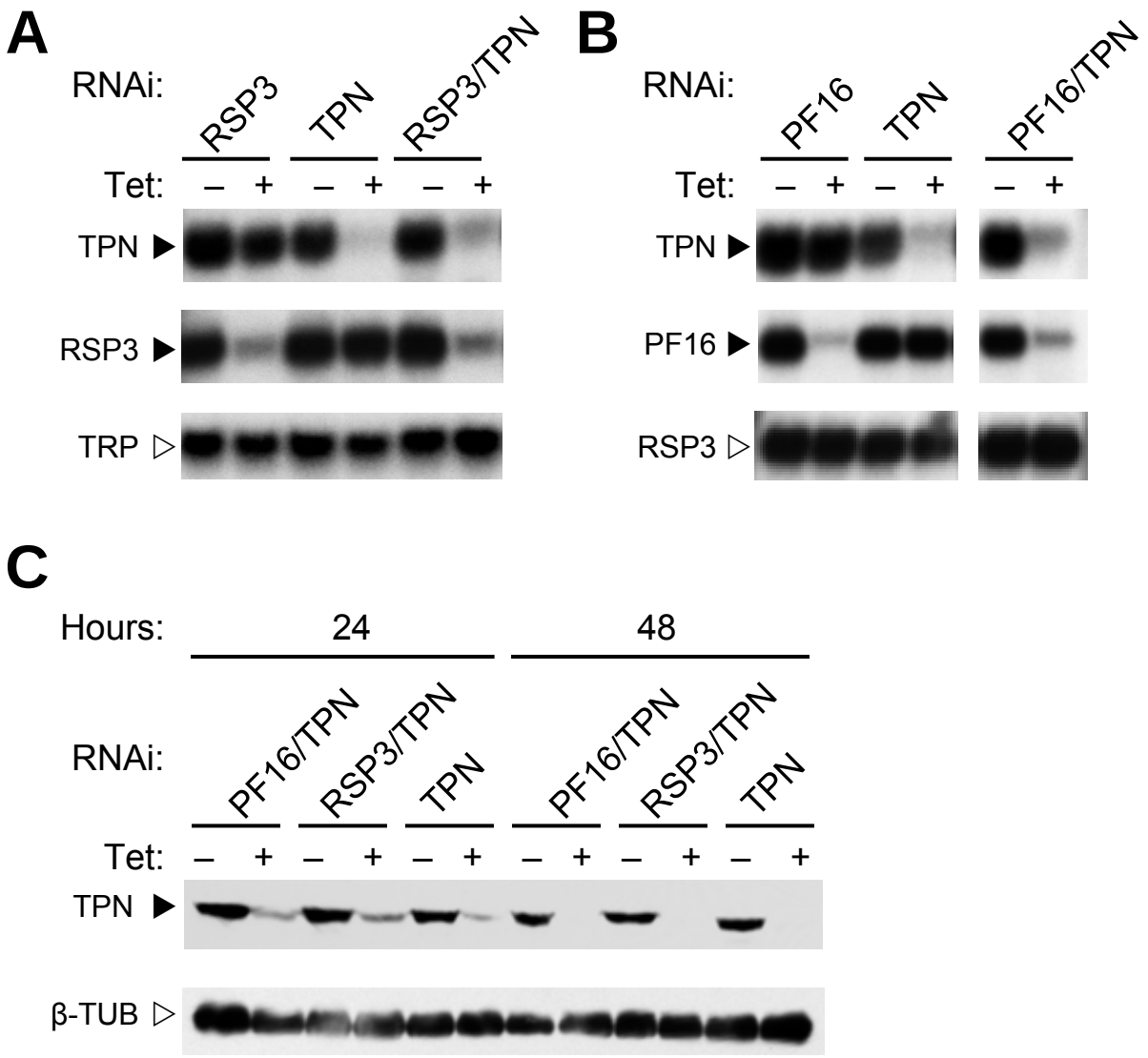
A
RNAi:
RSP3
TPN
RSP3/TPN
Tet: – + – + – +
TPN ▶
RSP3 ▶
TRP ▷
B
RNAi:
PF16
TPN
PF16/TPN
Tet: – + – + – +
TPN ▶
PF16 ▶
RSP3 ▷
C
Hours:
24
48
RNAi:
PF16/TPN
RSP3/TPN
TPN
PF16/TPN
RSP3/TPN
TPN
Tet: – + – + – + – + – + – +
TPN ▶
β-TUB ▷

Figure 8

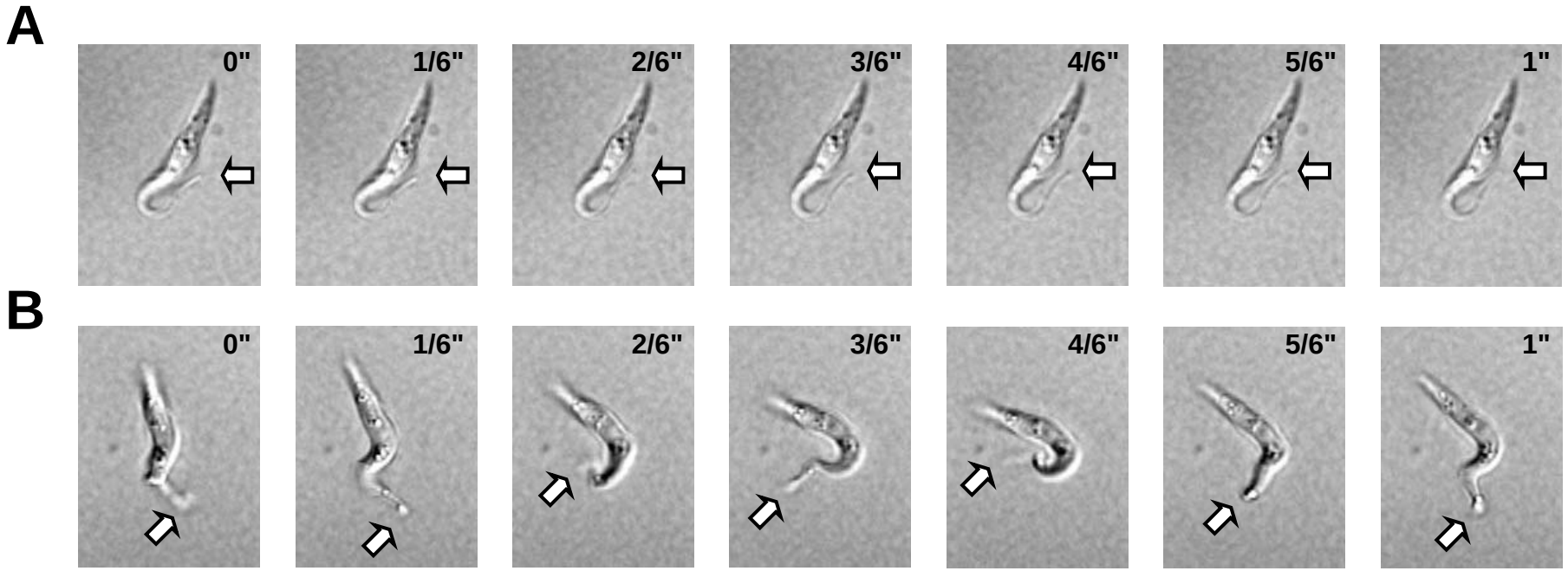
A
0"
1/6"
2/6"
3/6"
4/6"
5/6"
1"
B
0"
1/6"
2/6"
3/6"
4/6"
5/6"
1"

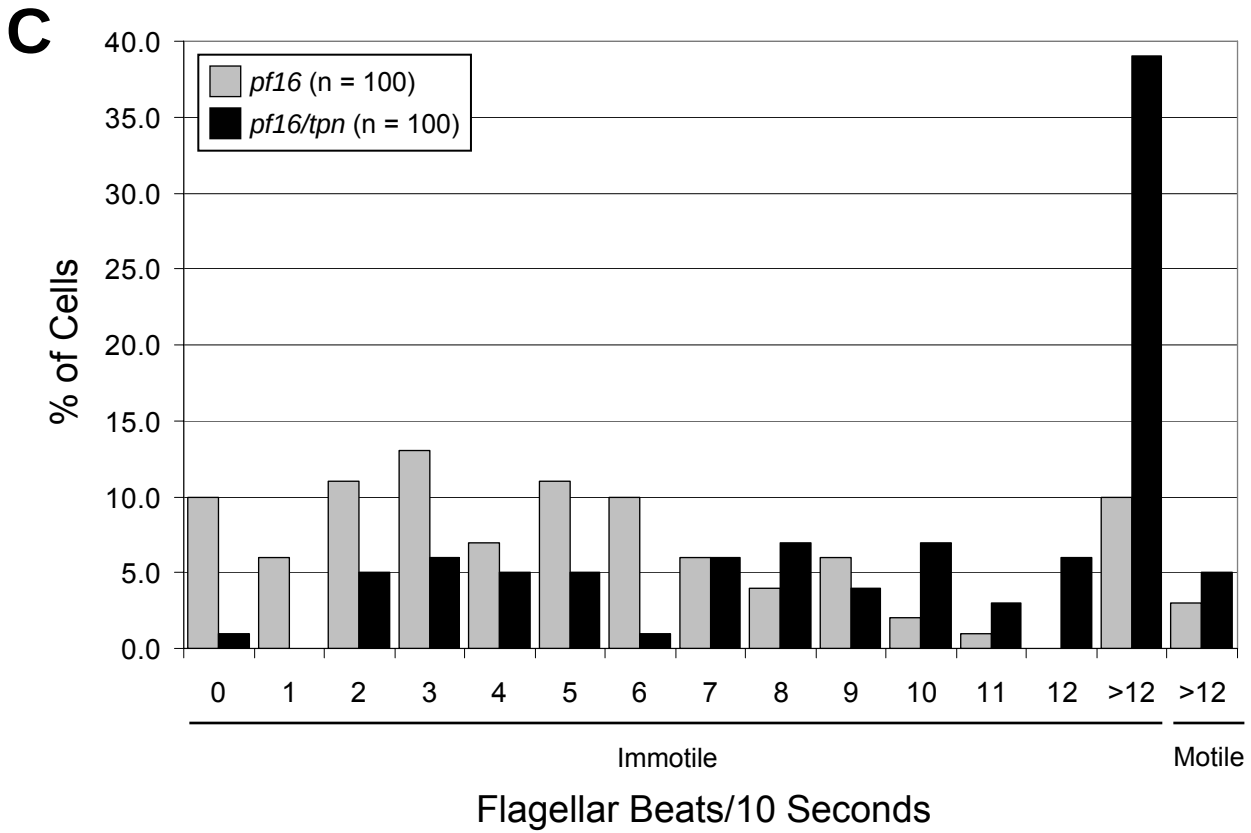
C
pf16 (n = 100)
pf16/tpn (n = 100)
% of Cells
40.0
35.0
30.0
25.0
20.0
15.0
10.0
5.0
0.0
0
1
2
3
4
5
6
7
8
9
10
11
12
>12
>12
Immotile
Motile
Flagellar Beats/10 Seconds

Table 1: Blind Assay of Single and Double Mutants

Mutant[a]	Cultures Correctly Identified[b]
Single (*pf16*)	20/22 (91%)
Double (*pf16/tpn)*	27/28 (96%)
Total	47/50 (94%)

[a] Four independent cultures of *pf16* single mutants (TbPF16) and *pf16/tpn* double mutants (TbPF16/TPN) were tetracycline-induced for 48 hours and were divided among 50 different culture flasks.

[b] Each of these 50 flasks were visually examined without knowledge of either the identity of the mutant (single or double), or how many flasks of each mutant were present. Samples were scored as single or double mutant, based on the phenotypic characteristics defined in the text.

Table 2: Cell motility and cytokinesis phenotypes

	Strain[a]			
	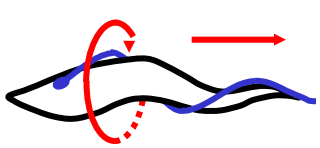	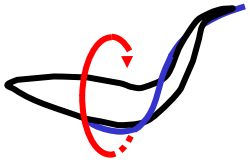		
Phenotype[b]	**Wild-type**	***tpn***	***pf16, pf20***	***pf16/tpn, rsp3, pfr2***
Flagellar Beat	+	+	-	+
Forward Motility	+	-	-	-
Cellular Rotation	+	+	-	-
Cytokinesis	+	+	-	-

[a] Schematic illustration of RNAi knockdown strains used in this study (*pf16*, *pf20*, *pf16/tpn*, *rsp3* and *pfr2*) as well as *tpn* knockdown (25) and wild-type strains. Flagella are shown in blue. A circular red arrow denotes cellular rotation and a straight red arrow denotes directional motility.

[b] Phenotypes of each strain, as described in the text. All mutants that are incapable of cellular rotation are also defective in cytokinesis.